Cell Reports

Modeling Type 1 Diabetes *In Vitro* Using Human Pluripotent Stem Cells

Graphical Abstract

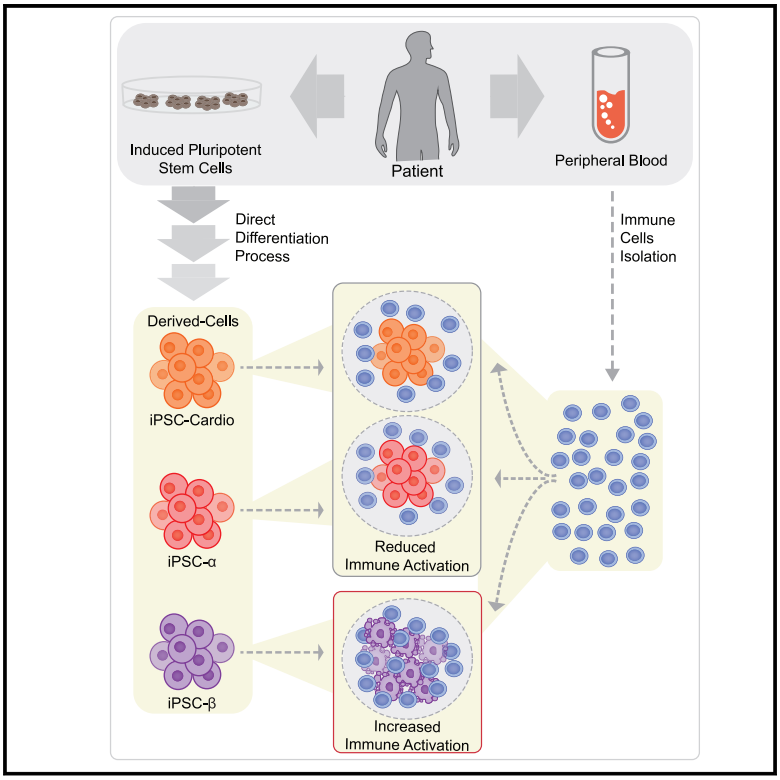

Highlights

- β cell-specific response is achieved using iPSC-β cells and autologous immune cells
- An *in vitro* immune response to iPSC-β cells requires ER stress
- T cell activation is restricted to autologous iPSC-β cells
- T cell activation is mediated by TCR engagement of peptide-HLA complexes on iPSC-β

Authors

Nayara C. Leite, Elad Sintov, Torsten B. Meissner, Michael A. Brehm, Dale L. Greiner, David M. Harlan, Douglas A. Melton

Correspondence

sintov@fas.harvard.edu (E.S.), dmelton@harvard.edu (D.A.M.)

In Brief

Leite et al. describe an *in vitro* platform that models features of autoimmune type 1 diabetes using patient-derived endocrine cells and autologous immune cells. This represents a path to developing a model with patient-derived cells to predict and analyze the autoimmune response.

Leite et al., 2020, Cell Reports *32*, 107894
July 14, 2020
https://doi.org/10.1016/j.celrep.2020.107894

Cell Reports

CellPress
OPEN ACCESS

Report

Modeling Type 1 Diabetes *In Vitro* Using Human Pluripotent Stem Cells

Nayara C. Leite,[1,7] Elad Sintov,[1,7,*] Torsten B. Meissner,[2,3] Michael A. Brehm,[4] Dale L. Greiner,[4] David M. Harlan,[5] and Douglas A. Melton[1,6,8,*]

[1]Department of Stem Cell and Regenerative Biology, Harvard Stem Cell Institute, Harvard University, Cambridge, MA 02138, USA
[2]Department of Surgery, Beth Israel Deaconess Medical Center, Boston, 02215 MA, USA
[3]Department of Medicine, Harvard Medical School, Boston, MA 02115, USA
[4]Program in Molecular Medicine, Diabetes Center of Excellence, University of Massachusetts Medical School, Worcester, MA 01655, USA
[5]Department of Medicine, Diabetes Center of Excellence, University of Massachusetts Medical School, Worcester, MA 01655, USA
[6]Howard Hughes Medical Institute, Chevy Chase, MD 20815, USA
[7]These authors contributed equally
[8]Lead Contact
*Correspondence: sintov@fas.harvard.edu (E.S.), dmelton@harvard.edu (D.A.M.)
https://doi.org/10.1016/j.celrep.2020.107894

SUMMARY

Understanding the root causes of autoimmune diseases is hampered by the inability to access relevant human tissues and identify the time of disease onset. To examine the interaction of immune cells and their cellular targets in type 1 diabetes, we differentiated human induced pluripotent stem cells into pancreatic endocrine cells, including β cells. Here, we describe an *in vitro* platform that models features of human type 1 diabetes using stress-induced patient-derived endocrine cells and autologous immune cells. We demonstrate a cell-type-specific response by autologous immune cells against induced pluripotent stem cell-derived β cells, along with a reduced effect on α cells. This approach represents a path to developing disease models that use patient-derived cells to predict the outcome of an autoimmune response.

INTRODUCTION

Type 1 diabetes (T1D) results from an autoimmune destruction of insulin-secreting pancreatic β cells (World Health Organization, 2016). Genetic and environmental factors may render β cells susceptible to attack by the immune system and contribute to β cell dysfunction (van Belle et al., 2011; Pugliese, 2013); however, the exact triggers and progression to clinical onset are not fully understood.

Insulin accounts for up to 50% of protein production in β cells, and this increases in response to metabolic demand (Scheuner and Kaufman, 2008; Schuit et al., 1988). Consequently, β cells are prone to endoplasmic reticulum (ER) stress and protein misfolding that can lead to β cell failure (Engin, 2016). It has also been suggested that the onset of T1D is associated with viral infection (Hober and Sauter, 2010), β cell exposure to chemicals (Like and Rossini, 1976), reactive oxygen species (Delmastro and Piganelli, 2011), and inflammation (Eizirik et al., 2013). All of these environmental triggers can cause β cell ER stress, suggesting that ER stress may be a common factor in disease onset.

T1D was a lethal disease until the discovery of insulin in the 1920s, and since then, insulin injection remains the primary treatment for T1D patients (Banting et al., 1922). The transplantation of cadaveric islets along with immunosuppression has been successfully performed to treat T1D (Shapiro et al., 2000). The challenges associated with transplantation, including the paucity of available human islets and allogeneic immune responses, may be overcome through the use of patient induced pluripotent stem cell-derived β cells (iPSC-β). Human iPSC-β cells could have the potential to replace the function of the β cells lost in T1D (Pagliuca et al., 2014; Veres et al., 2019; Nair et al., 2019; Russ et al., 2015; Rezania et al., 2014), thereby reducing or eliminating the need for exogenous insulin. However, it is expected that autologous iPSC-β cells will still be vulnerable to recurrent autoimmunity following transplantation (Sutherland et al., 1984; Sibley et al., 1985). Immune evasion strategies, including encapsulation with biomaterials or genetic manipulation, represent ways forward in advancing iPSC-β cell transplant therapies. Developing such strategies would benefit from a model that can predict tissue rejection in T1D patients. Here, we describe an *in vitro* platform using iPSC-β and iPSC-α cells that recapitulates some aspects of the autologous immune interaction in human T1D. This platform makes it possible to more intently study human autoimmune interactions and may be used for immunogenic evaluation before cell replacement therapy.

RESULTS

Immune Profiling of *In Vitro*-Generated Patient-Derived β and α Cells

iPSCs were derived from three T1D donor (T1D$^{1-3}$) and one non-T1D (ND) donor (Figure 1A; Table S1). After iPSC characterization (Figures S1A and 1B), cells were differentiated *in vitro* using two different protocols to produce islet-like clusters that are

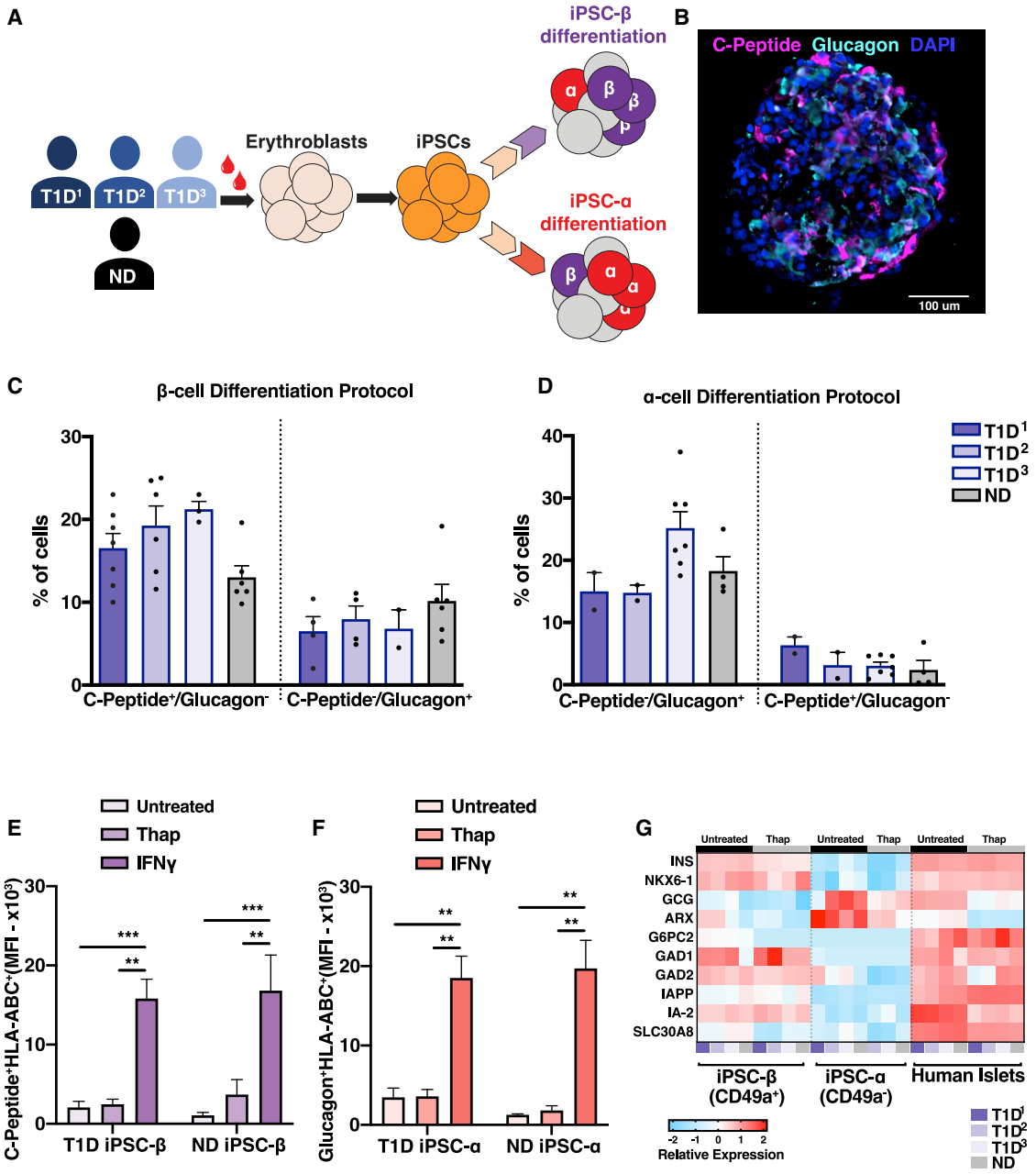

Figure 1. Immune Profiling of *In Vitro*-Generated Patient-Derived β and α Cells

(A) Schematic of the differentiation workflow.

(B) Immunostaining of an iPSC-β cluster.

(C and D) Flow cytometry quantification of C-peptide- and glucagon-positive cells in the β-cell differentiation protocol (C) and α-cell differentiation protocol (C). n = 3 T1D and n = 1 ND donor, n = 3–7 differentiation batches per donor line.

(E and F) Flow cytometry quantification of HLA-A, -B, and -C iPSC-β clusters treated with thap (5 μM for 5 h) or IFNγ (100 U/mL, 48 h), gated on C-peptide-positive cells (E) and glucagon-positive cells (F). The values are represented as adjusted mean fluorescence intensity (MFI). n = 3 T1D and n = 1 ND donor, n = 3 differentiation batches per donor line. $T1D^1$, $T1D^2$, and $T1D^3$ were pooled together.

(G) Relative mRNA expression of T1D-associated autoantigens in clusters untreated or treated with thap (5 μM for 5 h). Each column represents a donor and each row represents a gene. n = 3 T1D, n = 1 ND donor, n = 4 control human islets.

**p < 0.01 and ***p < 0.0005. Ordinary 1-way ANOVA. ns, non-significant. See also Figure S1.

enriched in either insulin-producing iPSC-β cells (Veres et al., 2019) or glucagon-producing iPSC-α cells (Peterson et al., 2020) (β cell and α differentiation protocol, respectively) (Figure 1A). The efficiency of β or α cell generation varies between PSC lines, yet both the T1D and ND iPSC lines were able to differentiate into iPSC-β or iPSC-α clusters. The differentiation protocols produced ~20% of the desired cell type (Figures 1B–1D), similar to previous reports using iPSC lines (Millman et al., 2016). While these designations indicate the predominant endocrine cell type in each protocol, iPSC-β clusters also have glucagon-producing α cells (10%) and vice versa (5%) (Figures 1B–1D, S1C, and S1D). These iPSC-β and -α cell-enriched preparations were used as autologous targets for immune studies, with peripheral blood mononuclear cells (PBMCs) isolated from the corresponding donors.

Little is known about the immunogenicity of iPSC-β or iPSC-α cells (van der Torren et al., 2017). The human leukocyte antigen complex (HLA) gene locus is the top risk allele in T1D (Pociot, 2017), and HLA expression is required for a robust adaptive immune response (Clark et al., 2017). Since our goal was to recapitulate immune interactions that may occur in T1D pathogenesis, we investigated the expression of molecules relevant to T cell recognition in iPSC-β and iPSC-α from T1D and ND donors in stress conditions. The iPSC-α and -β cell preparations were treated with soluble interferon gamma (IFNγ) to mimic inflammatory stress and thapsigargin (thap) to induce ER stress (Kracht et al., 2017; Marre et al., 2018). Following IFNγ (Richardson et al., 2016) but not by thap treatment alone, iPSC-β and iPSC-α cells upregulated HLA class I (HLA-ABC) and other immunoregulatory molecules, including programmed death-ligand 1 (PD-L1) and Fas cell surface death receptor (FasR) (see Figures S1G–S1P, 1E, and 1F). The expression of molecules relevant to immune recognition was similar in both ND and T1D iPSC-α and -β cells. The IFNγ-induced upregulated HLA-ABC protein expression was the same between iPSC-β cells and human islets following cytokine treatment. The HLA-ABC expression was lower in resting iPSC-α and -β cells compared to control islets (Figure S1Q).

Several islet proteins have been identified as targets of autoimmunity in T1D, including proinsulin (*INS*), glutamic acid decarboxylase (*GAD*), tyrosine phosphatase-like insulinoma-associated antigen 2 (IA-2, *PTPRN*), islet-specific glucose-6-phosphatase catalytic subunit–related protein (*G6PC2*), the cation efflux transporter ZNT8 (*SLC30A8*), islet-amyloid polypeptide (*IAPP*), and others (Pugliese, 2017). CD8 T cell epitopes from these proteins have been identified in the PBMCs of recent-onset T1D patients, suggesting a role in β cell destruction (Velthuis et al., 2010). We determined the relative transcript expression encoding these protein targets in derived iPSC-β or -α cells. We found similar levels of mRNA in iPSC-β cells, albeit low in some cases, for *G6PC2*, *SLC30A8*, *IAPP*, *INS*, *GAD,* and *IA-2* in both T1D and ND iPSC-β cells and in islets isolated from a control donor (Figure 1G).

T Cells Are Activated When Co-cultured with Autologous ER-Stressed iPSC-β Cells

To examine the interaction between iPSC-β and immune cells, we co-cultured autologous PBMCs with their corresponding iPSC-β cell clusters. Immune activation was evaluated by surface staining of T cell activation markers and by cytokine secretion after a 48-h co-culture.

We assessed the immune response of autologous PBMCs when co-cultured with iPSC-β clusters from ND and T1D donors (Figure 2A). As a positive control, PBMCs were stimulated with anti-CD3/CD28 beads (Figures S2A–S2C). T cell activation was not observed when autologous PBMCs were co-cultured with the corresponding untreated iPSC-endocrine cells (Figure 2). Similarly, iPSC-β pre-stimulated with IFNγ to enhance antigen presentation did not elicit an immune response (Figures S2E and S2F). Previous studies have reported that β cell ER stress has implications for immunogenicity in T1D. ER stress has been shown to increase β cell immunogenicity and can lead to T1D (Eizirik et al., 2008). To mimic ER stress, iPSC-β cells were pre-treated with thapsigagin (thap) for 5 h before co-culturing with PBMCs for 48 h. Thap treatment of PBMCs alone did not induce T cell activation (Figure S2D).

Co-culturing PBMCs with autologous T1D and ND iPSC-β, pre-treated with thap, resulted in upregulated immune cell activation markers CD25 and CD69 on T cell populations (Figures 2B, 2C, and S2G) and in increased levels of IFNγ, interleukin-2 (IL-2), IL-17, and C-X-C motif ligand 10 (CXCL10) (Figure 2D). Both CD69, a type II C-lectin receptor, and CD25, the high-affinity IL-2 receptor-α chain, are early activation markers expressed rapidly by human conventional CD8 and CD4 T cells following T cell receptor (TCR) engagement (Cibrián and Sánchez-Madrid, 2017; Caruso et al., 1997). We also observed a decrease in viable iPSC-β in the thap-treated co-culture experiments (Figures 2E and S4G). These results support a causal role of ER stress in eliciting an immune response, as previously reported by others. Autologous co-culture with iPSC-β with PBMCs induced an immune response in both T1D donors and ND donors. These observations are in line with reports describing that islet-reactive T cell frequencies in the blood do not distinguish T1D from ND individuals (Culina et al., 2018).

Next, we performed experiments to determine whether the observed T cell activation within the PBMCs is mediated by direct TCR engagement with the HLA complex on iPSC-β cells, rather than a T cell bystander activation caused by the inflammatory cytokine milieu or engagement of co-stimulatory molecules by other cells present in the PBMCs. First, the iPSC-β target cells were pre-treated with an HLA class I blocking antibody to prevent TCR binding to the peptide-HLA complex (Figures 3A, 3B, S3A, and S3D). Second, we used a transwell co-culture system that precludes contact between the immune cells and iPSC-β (Figure 3C). Third, iPSCs were transduced with a B2M guide RNA and Cas9, leading to the decreased expression of HLA class I on differentiated iPSC-β cells (Figures 3D, S3B, and S3C). In all three experiments, reduced T cell activation was assessed by cytokine secretion and evaluation of the T cell activation markers CD25 and CD69 in $CD8^+$ T cells present in the PBMCs. These results support the conclusion that T cell activation is mediated by direct TCR engagement of peptide-HLA complexes on iPSC-β.

Activation and Killing by T Cells Is Selective for iPSC-β

The main feature of T1D is selective destruction of pancreatic β, but not α, cells. To test whether the *in vitro* platform recapitulates

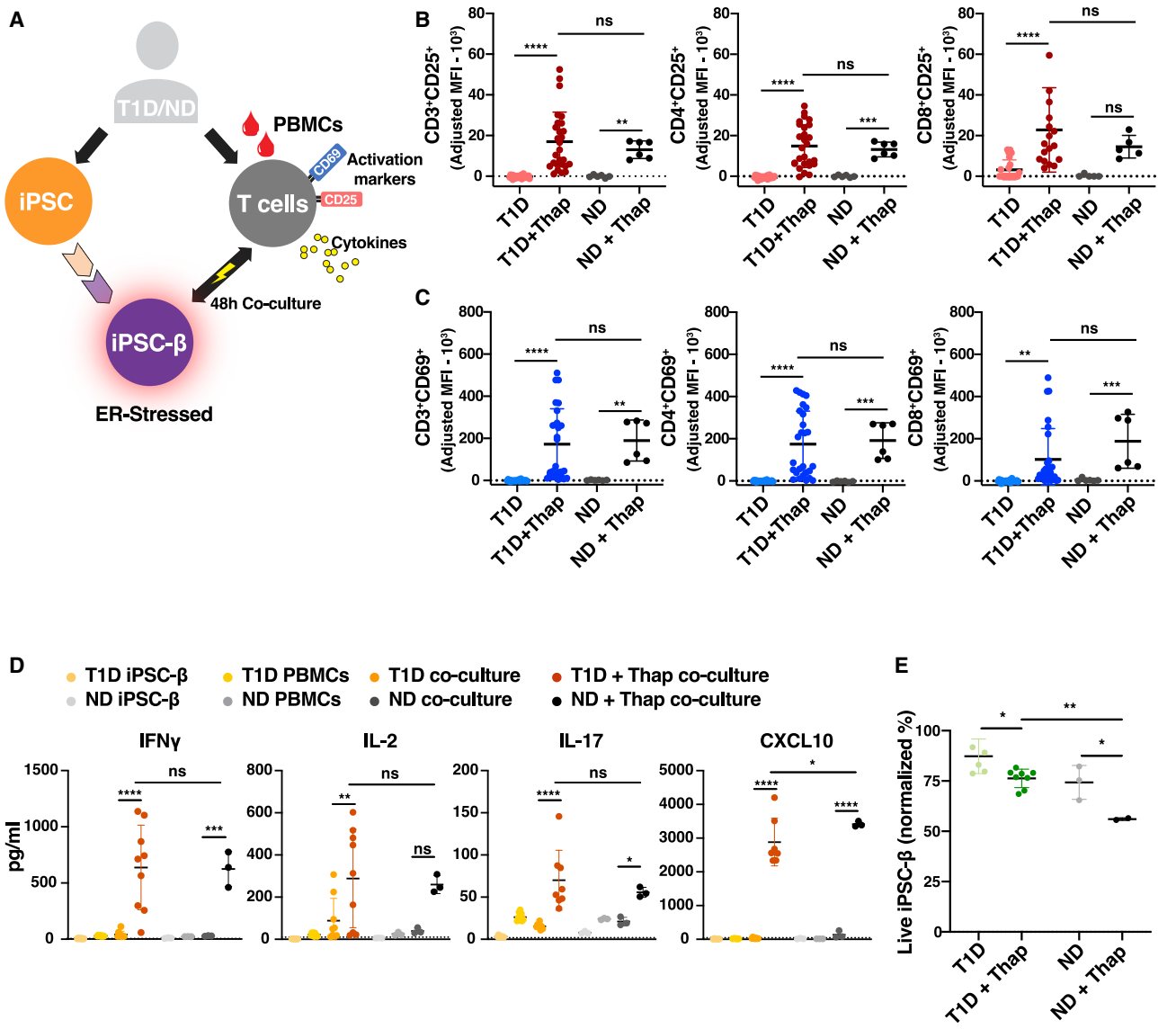

Figure 2. T Cells Are Activated When Co-cultured with Autologous ER-Stressed iPSC-β

(A) Experimental design: PBMCs co-cultured with autologous iPSC-β.

(B–D) Flow cytometry data of T cells after a 4-8h co-culture with iPSC-β cells (n = 3 T1D and n = 1 ND donor, n = 3 differentiation batches per donor line). $T1D^1$, $T1D^2$, and $T1D^3$ were pooled together.

(B) $CD25^+$ and (C) $CD69^+$ co-positive for $CD3^+$, $CD4^+$, or $CD8^+$ cells, as indicated. The values are represented as adjusted MFI.

(D) Pro-inflammatory cytokine detection in supernatants collected after 48 h co-culture of PBMC with iPSC-β (n = 3 T1D and n = 1 ND donor, n = 3 differentiation batches per donor line). $T1D^1$, $T1D^2$, and $T1D^3$ were pooled together.

(E) Percentage of live iPSC-β after co-culture, gated for C-peptide$^+$/glucagon$^-$ (n = 3 T1D and n = 1 ND donor, n = 3 differentiation batches per donor line). $T1D^1$, $T1D^2$, and $T1D^3$ were pooled together.

*p < 0.05, **p < 0.01, ***p < 0.0005, and ****p < 0.0001. Ordinary 1-way ANOVA. ns, non-significant. See also Figure S2.

that specificity, we generated additional iPSC-derived cell types—autologous iPSC-α cells and iPSC-cardiomyocytes—and performed co-culture experiments, as described above (Figure 4A). All of the cell preparations (iPSC-β, iPSC-α, and cardiomyocytes) were pre-treated with thap before co-culturing with PBMCs.

T cell activation was restricted to co-culture with autologous iPSC-β cells and not to other iPSC-derived cells (Figures 4B, 4C, 4F, S2G, and S4A–S4C). Since β cells are highly secretory cells and more likely to undergo ER stress, we set out to evaluate whether the T cell response induced by iPSC-β was due to the resistance of iPSC-α to ER stress. Both iPSC-β and -α cells showed an increase in ER stress-related proteins, PRKR-like ER kinase (PERK), protein disulfide isomerase (PDI), and binding immunoglobulin protein (BiP) after thap treatment, demonstrating that both cell types

CellPress
OPEN ACCESS

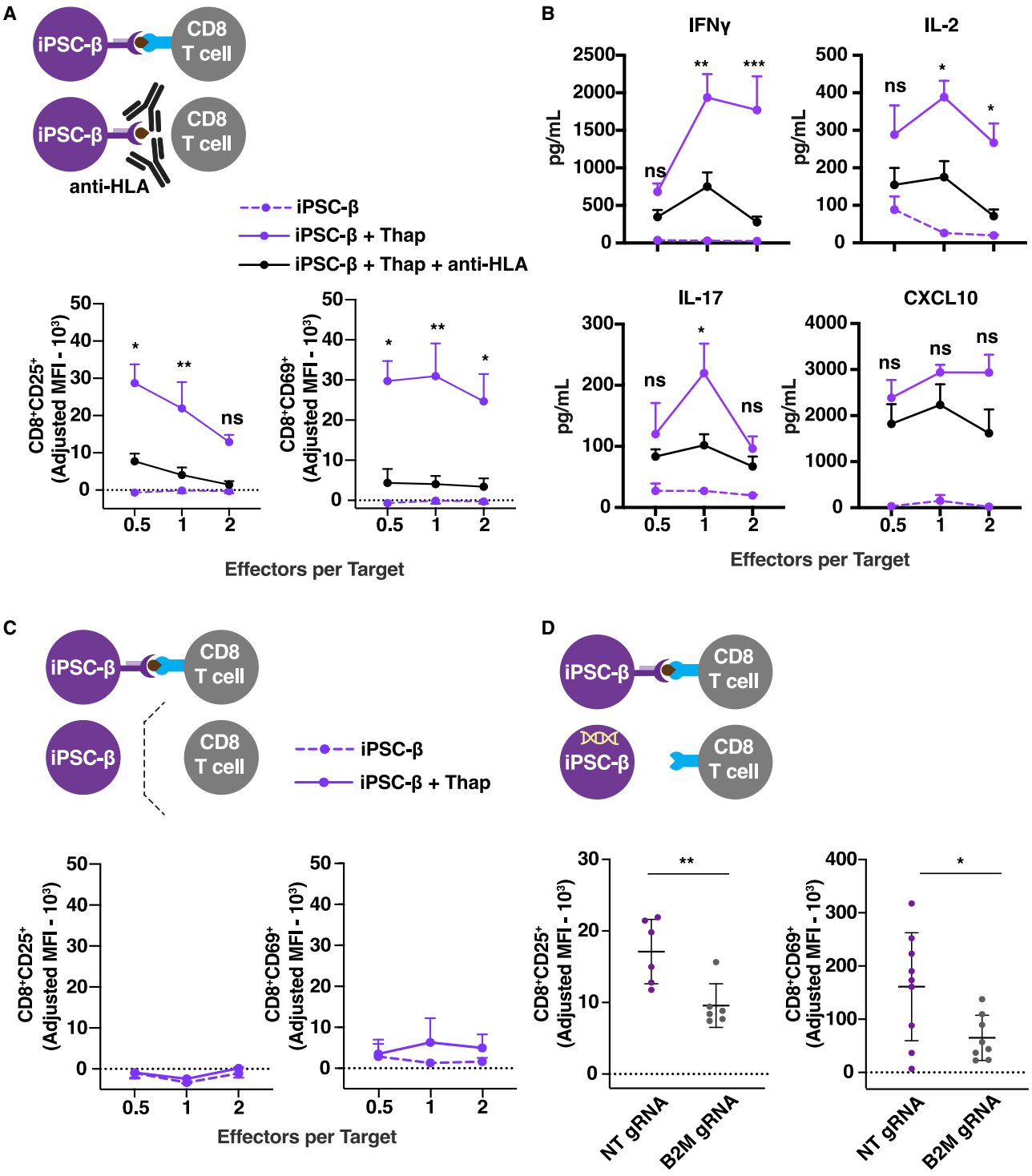

Figure 3. iPSC-β-Induced T Cell Activation and Killing Is Mediated by Direct T Cell-HLA Interaction

(A and B) PBMCs co-cultured for 48 h with autologous iPSC-β (n = 3 T1D donors, 3 differentiation batches per donor). iPSC-β were pre-treated with thap (5 μM for 5 h) and/or anti-HLA antibody for 30 min before co-culture.

(A) Flow cytometry after 48 h co-culture of T cell activation markers, $CD25^+$ and $CD69^+$, gated on $CD8^+$ cells.

(B) Pro-inflammatory cytokine detection in supernatants collected after 48 h co-culture of PBMCs with autologous iPSC-β ± thap.

(C) Expression of $CD25^+$ and $CD69^+$, gated on $CD8^+$ cells in a transwell system.

(legend continued on next page)

are sensitive to ER stress induction *in vitro* (Figures S1E and S1F).

To further explore iPSC-β cell specificity, we investigated whether iPSC-α cells are protected from T cell-mediated destruction compared to iPSC-β cells after autologous co-culture with PBMCs. We compared β and α cell numbers from their respective differentiation protocols (α versus β differentiation protocol) using two assays for survival after autologous co-culture with PBMCs: the percentage of live α and β cells by live cell count (Figures 4D, S4E, and S4F) and assessing apoptosis using the apopxin dye (Figures 4E and S4G). We found that fewer iPSC-β cells survive co-culture with autologous PBMCs compared to iPSC-α cells, and more iPSC-β cells are apoptotic compared to iPSC-α cells.

Since we observed a low activation of autologous immune cells in the presence of iPSC-α cells, we performed a co-culture experiment using unmatched PBMCs to test whether iPSC-α can induce an allogeneic T cell response. Allogeneic T cells upregulated the activation markers after co-culture with iPSC-α cells (Figure 4G). These results show that iPSC-α cells can be immunogenic and induce T cell reactivity in an allogeneic setting.

Our *in vitro* differentiation system generates a mixed population of endocrine cells. It is thus difficult to demonstrate whether the effects are cell specific or dependent on other cell types in the preparation. To address the question of β cell specificity, we used anti-CD49a staining to sort out iPSC-β cells. The negative fraction of the CD49a sorted cells was stained with CD26 to sort iPSC-α cells (Veres et al., 2019). This two-step method yields clusters of up to 80% β cells by CD49a sorting and up to 50% α cells by CD26 sorting (Figure S4D). After enriching both β and α cell populations, we performed co-culture experiments comparing both enriched populations and the original mixed population derived from the standard iPSC-β protocol. Co-culture with both enriched and standard iPSC-β cell clusters has similar levels of T cell activation while the α cell population induced minimal activation (Figure 4H). In summary, we show that an autoreactive, β cell-specific response can be achieved *in vitro* using iPSC-β cells and autologous immune cells, recapitulating key features of T1D.

DISCUSSION

A deeper understanding of the immunopathogenesis of T1D, including how it differs among T1D individuals, is needed to develop rational strategies to find a cure or to prevent the disease. Recent advances in stem cell technologies and access to patient samples provide the means to explore T1D pathogenesis. We established an *in vitro* platform using iPSC-derived pancreatic endocrine cells and autologous immune cells that recapitulates key aspects of T1D. We demonstrate that the immune response to β cells requires ER stress, that a direct, physical interaction between the T cells and β cells is necessary, and the T cell-mediated activation and killing is preferential to β cells, but not α cells.

The findings of this research should be interpreted in light of two major limitations. First, these experiments required the use of blood provided from the same patient who supplied the iPSCs used to generate iPSC-derived cells. We had to synchronize the time of cell generation with donor availability to obtain blood to perform the experiments. Second, cell numbers are a limitation for the co-culture experiments, since we were only able to isolate on average 50 million PBMCs from each blood draw. The approach would be strengthened by improving techniques to select and culture circulating pancreatic β cell-reactive immune cells. A better source of pancreatic β cell-reactive immune cells may be the draining pancreatic lymph nodes in T1D patients, but these are not readily accessible.

We observed unexpected results, including the activation of T cells by ND iPSC-β cells, the inability of IFNγ to induce an immune response, apart from HLA class I upregulation, and the requirement of ER stress to induce autologous T cell activation. We believe that iPSC-β cells mimic healthy β cells after reprogramming from somatic cells, regardless of whether they were derived from a T1D or a ND donor, thus putting both T1D and ND iPSC-β cells on the same starting line. To mimic a β cell disease state, we had to induce ER stress in the iPSC-β cells. This supports the idea that the trigger of β cell destruction in T1D is enhanced β cell vulnerability caused by islet inflammation due to ER stress. We did not observe any difference in the ability of iPSC-β cells from T1D donors to stimulate an immune response relative to iPSC-β cells from ND donors, and in either case, the cells had to be subjected to ER stress to promote an immune response. It is perhaps relevant that the pancreata of individuals with T1D are significantly smaller than those studied from ND individuals (Regnell et al., 2016; Virostko et al., 2019), and even that first-degree relatives of an index case with T1D have smaller pancreata (Campbell-Thompson et al., 2019). While conjectural, it stands to reason that a metabolic load imposed on pancreatic β cells will be greater per β cell when there are fewer such cells to carry the load.

We observed that T cell activation was restricted to co-culture with the autologous iPSC-β cell preparation and not to the iPSC-α or cardiomyocyte preparation. iPSC-β cells expressed genes encoding peptides associated with T1D. Although we did not assess natural processing and presentation or verify peptide modification in the iPSC-derived cells, $CD8^+$ T cells within PBMCs responded to stressed iPSC-β, suggesting that β cell-specific epitopes were generated. The importance of ER stress and the unfolded protein response in β cell pathophysiology and the autoimmune responses in T1D are not well understood (Marre et al., 2018; Eizirik et al., 2008). Our results add to this narrative by showing that ER stress in β cells is an important trigger for an immune response *in vitro*. Experiments using

(D) Expression of the activation marker $CD25^+$ and $CD69^+$ on $CD8^+$ cells after 48-h co-culture with autologous iPSC-β transduced with a lentivirus vector expressing a non-targeting (NT) or B2M guide RNA (gRNA) and Cas9 (n = 3 T1D donors, n = 3 differentiation batches per donor line). *p < 0.05 and **p < 0.01, Student's t test. $T1D^1$, $T1D^2$, and $T1D^3$ were pooled together. ns, non-significant.

(A–C) n = 3 T1D donors, n = 3 differentiation batches per donor line. $T1D^1$, $T1D^2$, and $T1D^3$ were pooled together. *p < 0.05, **p < 0.005, and ***p < 0.0005; 2-way ANOVA.

See also Figure S3.

CellPress
OPEN ACCESS

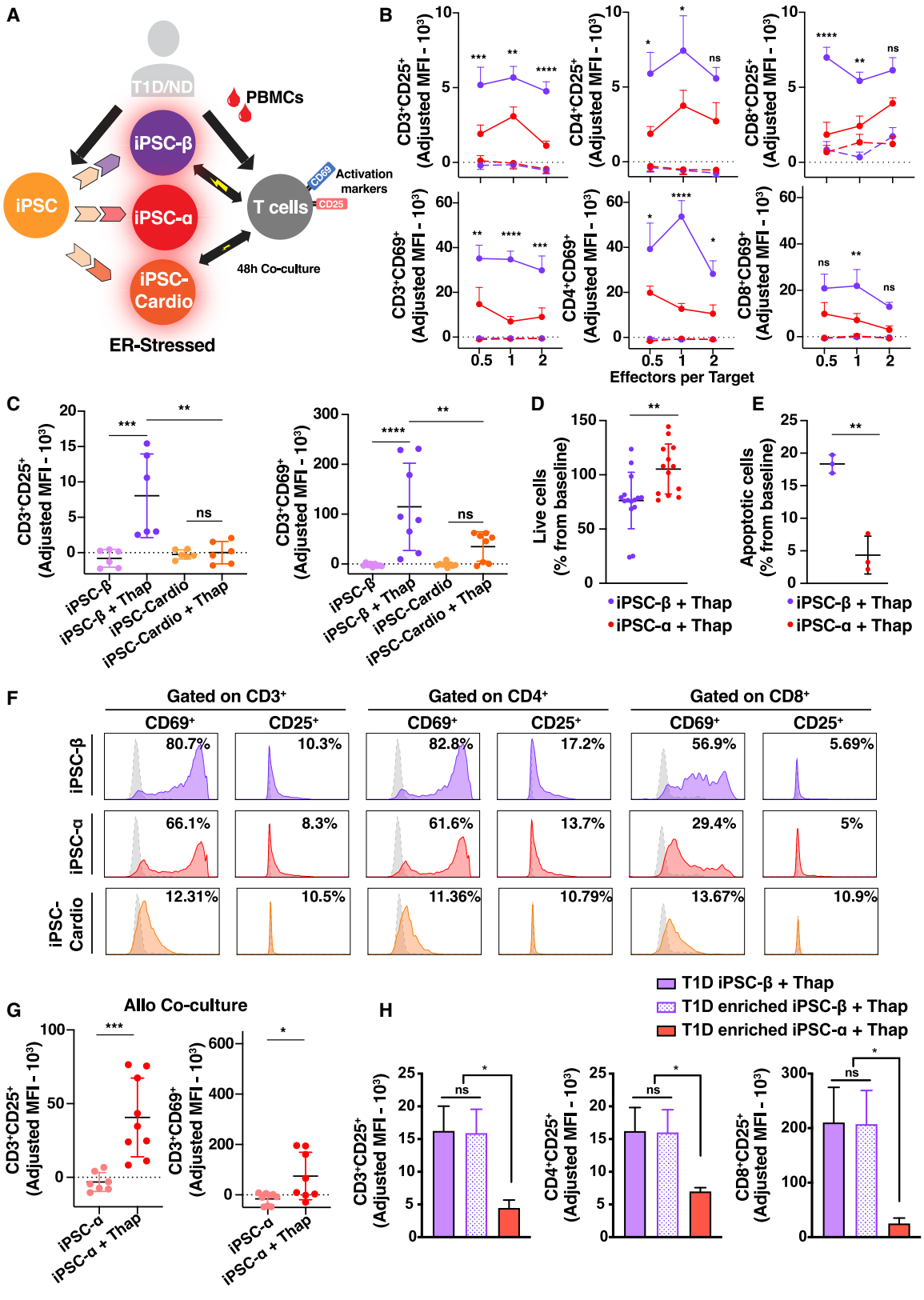

(legend on next page)

islet-specific T cell lines would take advantage of the system presented here and potentially strengthen the analysis and conclusions. It is unfortunate that the coronavirus disease 2019 (COVID-19) pandemic lockdown eliminated the possibility of obtaining the necessary patient blood samples for months, and we therefore could not perform these experiments. Our protocol for assessing antigen-specific T cell activation was the expression of both CD25 and CD69 on T cells (Caruso et al., 1997). A significant proportion of both CD8 and CD4 T cells are positive for CD69 expression, which may reflect the increased levels of inflammatory cytokines detected within the cultures. In contrast, expression of CD25 by human conventional CD8 and CD4 T cells is a better measure of antigen-specific stimulation of T cells and less likely to be significantly upregulated by cytokines alone (Shatrova et al., 2016). We postulate that the PBMC-iPSC-β cell co-cultures created an environment in which ER-stressed iPSC-β cells are presenting/releasing autoantigens and creating an inflammatory milieu that strongly stimulates autoreactive T cells to express CD25 and CD69 and that causes bystander T cells to upregulate CD69.

$CD8^+$ T cells play a fundamental role in T1D pathogenesis, as they take center stage in the destruction of pancreatic β cells and contribute to sustained islet inflammation (Coppieters et al., 2012). Although we also observed $CD4^+$ activation after co-culturing PBMCs and iPSC-β cells, we speculate that this activation is due to antigen presentation by professional antigen-presenting cells present in the PBMC preparation. However, we observed low levels of HLA-DR on iPSC-β that could be involved in HLA class II peptide presentation by β cells leading to $CD4^+$ T cell activation. Further investigation is necessary to elucidate the mechanism by which $CD4^+$s are activated in this system.

In summary, the *in vitro* platform described here can be used to better understand the cellular and molecular components relevant to immune cell interaction in human T1D. In addition, it opens the possibility of testing for the immune protection of tolerogenic engineered iPSC-β cells before cell replacement therapy. Genetically engineered iPSCs that evade immune destruction may ultimately reduce the need for harmful immunosuppression (Han et al., 2019; Deuse et al., 2019). Finally, our model can pave the way to the development of other disease models that take advantage of patient-derived cells to predict the outcome of an autoimmune response.

STAR★METHODS

Detailed methods are provided in the online version of this paper and include the following:

- KEY RESOURCES TABLE
- RESOURCE AVAILABILITY
  - Lead Contact
  - Materials Availability
  - Data and Code Availability
- EXPERIMENTAL MODEL AND SUBJECT DETAILS
- METHOD DETAILS
  - iPSC and PBMCs Derivation from Human Donors
  - Cell Culture
  - β Cell Differentiation Protocol
  - α Cell Differentiation Protocol
  - Magnetic enrichment using CD49a and CD26
  - Human Primary Immune Cell Isolation and Co-Culture Experiments
  - T Cell Activation Assay
  - Flow cytometry
  - Immunofluorescence Microscopy
  - Quantitative Real-time PCR (qPCR)
  - NanoString gene array
  - Protein Extraction and Immunoblotting
  - Cytokines Analysis
  - Viability and Apoptosis Assay
  - Lentivirus Preparation and Transduction
- QUANTIFICATION AND STATISTICAL ANALYSIS

SUPPLEMENTAL INFORMATION

Supplemental Information can be found online at https://doi.org/10.1016/j.celrep.2020.107894.

ACKNOWLEDGMENTS

We thank J. Babon, R. Pop, A.L. Faust, and K. Boulanger for discussions and feedback on the manuscript and the iPSC and Flow Cytometry Core Facilities at Harvard University for their support. D.A.M. is an Investigator of the Howard Hughes Medical Institute. N.C.L. is supported by American Diabetes Association grant #1-19-PMF-024. E.S. is supported by Juvenile Diabetes Research Foundation (JDRF) Post-Doctoral Fellowship (3-PDF-2018-590-A-N). This work was supported by grants from the Harvard Stem Cell Institute, the

Figure 4. Activation and Killing by T Cells Is Selective for iPSC-β

(A) Experimental design: PBMCs co-cultured with autologous iPSC-derived cells.

(B, C, and F) CD25 or CD69 expression shown as MFI.

(B) PBMCs (gated on $CD3^+$, $CD4^+$, and $CD8^+$ populations) co-cultured for 48 h with autologous iPSC-β (purple) or iPSC-α (red). (n = 3 T1D and n = 1 ND donor, n = 3 differentiation batches per donor line). $T1D^1$, $T1D^2$, and $T1D^3$ were pooled together.

(C) Donor-matched PBMCs ($CD3^+$ gated) (n = 1 T1D, n = 3 differentiation batches per donor line) co-cultured for 48 h with autologous iPSC-β (purple) or iPSC-cardiomyocytes (orange).

(D) Percentage of live iPSC-β (C-$peptide^+$/$glucagon^-$) or iPSC-α (C-$peptide^-$/$glucagon^+$) from iPSC-β or iPSC-α differentiations, respectively (n = 3 T1D donors, n = 3 differentiation batches per donor line). $T1D^1$, $T1D^2$, and $T1D^3$ were pooled together.

(F) Representative flow cytometry histograms after 48 h of co-culture. Dashed histogram represents the control (untreated target cells).

(E) Percentage of apoptotic ($apopxin^+$) iPSC-β ($CD49a^+$/$CD26^-$) or iPSC-α ($CD49a^-$/$CD26^+$) from iPSC-β or iPSC-α differentiations (n = 1 T1D iPSC donor, n = 3 differentiation batches per donor line).

(G) Unmatched PBMCs ($CD3^+$ gated cells) co-cultured for 48 h with iPSC-α (n = 3 T1D donors, n = 3 differentiation batches per donor line). $T1D^1$, $T1D^2$, and $T1D^3$ were pooled together.

(H) Donor-matched PBMCs (gated on $CD3^+$, $CD4^+$, and $CD8^+$ populations) co-cultured for 48 h with autologous enriched iPSC-β or iPSC-α.

Data are means ± SEMs, 2-way ANOVA. *$p < 0.05$, **$p < 0.005$, ***$p < 0.0005$, and ****$p < 0.0001$; ns, non-significant. See also Figure S4.

Helmsley Charitable Trust (2015PG-T1D044), JDRF (5-SRA-2014-284-Q-R), National Institutes of Health (NIH): NIH UO1DK104218, NIH R24OD0426640, and NIH UC4DK104218, and the JPB Foundation (award no. 1094).

AUTHOR CONTRIBUTIONS

N.C.L. and E.S. conceived the study. The experiments were performed by N.C.L. and E.S. T.B.M. provided technical support and conceptual advice. M.A.B., D.L.G., and D.M.H. were involved in the experimental design and patient recruitment and advised on the project. N.C.L., E.S., and D.A.M. wrote the manuscript. D.A.M. designed and supervised the research.

DECLARATION OF INTERESTS

D.A.M. is a founder of Semma Therapeutics and an advisor to Vertex, who have licensed technologies developed in the Melton lab. All of the other authors declare no competing interests.

Received: January 13, 2020
Revised: May 1, 2020
Accepted: June 21, 2020
Published: July 14, 2020

REFERENCES

Banting, F.G., Best, C.H., Collip, J.B., Campbell, W.R., and Fletcher, A.A. (1922). Pancreatic Extracts in the Treatment of Diabetes Mellitus. Can. Med. Assoc. J. *12*, 141–146.

Campbell-Thompson, M.L., Filipp, S.L., Grajo, J.R., Nambam, B., Beegle, R., Middlebrooks, E.H., Gurka, M.J., Atkinson, M.A., Schatz, D.A., and Haller, M.J. (2019). Relative Pancreas Volume Is Reduced in First-Degree Relatives of Patients With Type 1 Diabetes. Diabetes Care *42*, 281–287.

Caruso, A., Licenziati, S., Corulli, M., Canaris, A.D., De Francesco, M.A., Fiorentini, S., Peroni, L., Fallacara, F., Dima, F., Balsari, A., and Turano, A. (1997). Flow cytometric analysis of activation markers on stimulated T cells and their correlation with cell proliferation. Cytometry *27*, 71–76.

Cibrián, D., and Sánchez-Madrid, F. (2017). CD69: from activation marker to metabolic gatekeeper. Eur. J. Immunol. *47*, 946–953.

Clark, M., Kroger, C.J., and Tisch, R.M. (2017). Type 1 Diabetes: A Chronic Anti-Self-Inflammatory Response. Front. Immunol. *8*, 1898.

Coppieters, K.T., Dotta, F., Amirian, N., Campbell, P.D., Kay, T.W., Atkinson, M.A., Roep, B.O., and von Herrath, M.G. (2012). Demonstration of islet-autoreactive CD8 T cells in insulitic lesions from recent onset and long-term type 1 diabetes patients. J. Exp. Med. *209*, 51–60.

Culina, S., Lalanne, A.I., Afonso, G., Cerosaletti, K., Pinto, S., Sebastiani, G., Kuranda, K., Nigi, L., Eugster, A., Østerbye, T., et al.; ImMaDiab Study Group (2018). Islet-reactive $CD8^+$ T cell frequencies in the pancreas, but not in blood, distinguish type 1 diabetic patients from healthy donors. Sci. Immunol. *3*, eaao4013.

Delmastro, M.M., and Piganelli, J.D. (2011). Oxidative stress and redox modulation potential in type 1 diabetes. Clin. Dev. Immunol. *2011*, 593863.

Deuse, T., Hu, X., Gravina, A., Wang, D., Tediashvili, G., De, C., Thayer, W.O., Wahl, A., Garcia, J.V., Reichenspurner, H., et al. (2019). Hypoimmunogenic derivatives of induced pluripotent stem cells evade immune rejection in fully immunocompetent allogeneic recipients. Nat. Biotechnol. *37*, 252–258.

Eizirik, D.L., Cardozo, A.K., and Cnop, M. (2008). The role for endoplasmic reticulum stress in diabetes mellitus. Endocr. Rev. *29*, 42–61.

Eizirik, D.L., Miani, M., and Cardozo, A.K. (2013). Signalling danger: endoplasmic reticulum stress and the unfolded protein response in pancreatic islet inflammation. Diabetologia *56*, 234–241.

Engin, F. (2016). ER stress and development of type 1 diabetes. J. Investig. Med. *64*, 2–6.

Han, X., Wang, M., Duan, S., Franco, P.J., Kenty, J.H., Hedrick, P., Xia, Y., Allen, A., Ferreira, L.M.R., Strominger, J.L., et al. (2019). Generation of hypoimmunogenic human pluripotent stem cells. Proc. Natl. Acad. Sci. USA *116*, 10441–10446.

Hober, D., and Sauter, P. (2010). Pathogenesis of type 1 diabetes mellitus: interplay between enterovirus and host. Nat. Rev. Endocrinol. *6*, 279–289.

Kracht, M.J., van Lummel, M., Nikolic, T., Joosten, A.M., Laban, S., van der Slik, A.R., van Veelen, P.A., Carlotti, F., de Koning, E.J., Hoeben, R.C., et al. (2017). Autoimmunity against a defective ribosomal insulin gene product in type 1 diabetes. Nat. Med. *23*, 501–507.

Like, A.A., and Rossini, A.A. (1976). Streptozotocin-induced pancreatic insulitis: new model of diabetes mellitus. Science *193*, 415–417.

Marre, M.L., McGinty, J.W., Chow, I.T., DeNicola, M.E., Beck, N.W., Kent, S.C., Powers, A.C., Bottino, R., Harlan, D.M., Greenbaum, C.J., et al. (2018). Modifying Enzymes Are Elicited by ER Stress, Generating Epitopes That Are Selectively Recognized by $CD4^+$ T Cells in Patients With Type 1 Diabetes. Diabetes *67*, 1356–1368.

Millman, J.R., Xie, C., Van Dervort, A., Gürtler, M., Pagliuca, F.W., and Melton, D.A. (2016). Generation of stem cell-derived β-cells from patients with type 1 diabetes. Nat. Commun. *7*, 11463.

Nair, G.G., Liu, J.S., Russ, H.A., Tran, S., Saxton, M.S., Chen, R., Juang, C., Li, M.L., Nguyen, V.Q., Giacometti, S., et al. (2019). Recapitulating endocrine cell clustering in culture promotes maturation of human stem-cell-derived β cells. Nat. Cell Biol. *21*, 263–274.

Pagliuca, F.W., Millman, J.R., Gürtler, M., Segel, M., Van Dervort, A., Ryu, J.H., Peterson, Q.P., Greiner, D., and Melton, D.A. (2014). Generation of functional human pancreatic β cells in vitro. Cell *159*, 428–439.

Peterson, Q.P., Veres, A., Chen, L., Slama, M.Q., Kenty, J.H.R., Hassoun, S., Brown, M.R., Dou, H., Duffy, C.D., Zhou, Q., et al. (2020). A method for the generation of human stem cell-derived alpha cells. Nat. Commun. *11*, 2241.

Pociot, F. (2017). Type 1 diabetes genome-wide association studies: not to be lost in translation. Clin. Transl. Immunology *6*, e162.

Pugliese, A. (2013). The multiple origins of Type 1 diabetes. Diabet. Med. *30*, 135–146.

Pugliese, A. (2017). Autoreactive T cells in type 1 diabetes. J. Clin. Invest. *127*, 2881–2891.

Regnell, S.E., Peterson, P., Trinh, L., Broberg, P., Leander, P., Lernmark, Å., Månsson, S., and Elding Larsson, H. (2016). Pancreas volume and fat fraction in children with Type 1 diabetes. Diabet. Med. *33*, 1374–1379.

Rezania, A., Bruin, J.E., Arora, P., Rubin, A., Batushansky, I., Asadi, A., O'Dwyer, S., Quiskamp, N., Mojibian, M., Albrecht, T., et al. (2014). Reversal of diabetes with insulin-producing cells derived in vitro from human pluripotent stem cells. Nat. Biotechnol. *32*, 1121–1133.

Richardson, S.J., Rodriguez-Calvo, T., Gerling, I.C., Mathews, C.E., Kaddis, J.S., Russell, M.A., Zeissler, M., Leete, P., Krogvold, L., Dahl-Jørgensen, K., et al. (2016). Islet cell hyperexpression of HLA class I antigens: a defining feature in type 1 diabetes. Diabetologia *59*, 2448–2458.

Russ, H.A., Parent, A.V., Ringler, J.J., Hennings, T.G., Nair, G.G., Shveygert, M., Guo, T., Puri, S., Haataja, L., Cirulli, V., et al. (2015). Controlled induction of human pancreatic progenitors produces functional beta-like cells in vitro. EMBO J. *34*, 1759–1772.

Sanjana, N.E., Shalem, O., and Zhang, F. (2014). Improved vectors and genome-wide libraries for CRISPR screening. Nat. Methods *11*, 783–784.

Scheuner, D., and Kaufman, R.J. (2008). The unfolded protein response: a pathway that links insulin demand with beta-cell failure and diabetes. Endocr. Rev. *29*, 317–333.

Schuit, F.C., In't Veld, P.A., and Pipeleers, D.G. (1988). Glucose stimulates proinsulin biosynthesis by a dose-dependent recruitment of pancreatic beta cells. Proc. Natl. Acad. Sci. USA *85*, 3865–3869.

Shapiro, A.M., Lakey, J.R., Ryan, E.A., Korbutt, G.S., Toth, E., Warnock, G.L., Kneteman, N.M., and Rajotte, R.V. (2000). Islet transplantation in seven patients with type 1 diabetes mellitus using a glucocorticoid-free immunosuppressive regimen. N. Engl. J. Med. *343*, 230–238.

Shatrova, A.N., Mityushova, E.V., Vassilieva, I.O., Aksenov, N.D., Zenin, V.V., Nikolsky, N.N., and Marakhova, I.I. (2016). Time-Dependent Regulation of IL-2R α-Chain (CD25) Expression by TCR Signal Strength and IL-2-Induced STAT5 Signaling in Activated Human Blood T Lymphocytes. PLOS ONE *11*, e0167215.

Sibley, R.K., Sutherland, D.E., Goetz, F., and Michael, A.F. (1985). Recurrent diabetes mellitus in the pancreas iso- and allograft. A light and electron microscopic and immunohistochemical analysis of four cases. Lab. Invest. *53*, 132–144.

Sutherland, D.E., Sibley, R., Xu, X.Z., Michael, A., Srikanta, A.M., Taub, F., Najarian, J., and Goetz, F.C. (1984). Twin-to-twin pancreas transplantation: reversal and reenactment of the pathogenesis of type I diabetes. Trans. Assoc. Am. Physicians *97*, 80–87.

van Belle, T.L., Coppieters, K.T., and von Herrath, M.G. (2011). Type 1 diabetes: etiology, immunology, and therapeutic strategies. Physiol. Rev. *91*, 79–118.

van der Torren, C.R., Zaldumbide, A., Duinkerken, G., Brand-Schaaf, S.H., Peakman, M., Stangé, G., Martinson, L., Kroon, E., Brandon, E.P., Pipeleers, D., and Roep, B.O. (2017). Immunogenicity of human embryonic stem cell-derived beta cells. Diabetologia *60*, 126–133.

Velthuis, J.H., Unger, W.W., Abreu, J.R., Duinkerken, G., Franken, K., Peakman, M., Bakker, A.H., Reker-Hadrup, S., Keymeulen, B., Drijfhout, J.W., et al. (2010). Simultaneous detection of circulating autoreactive CD8+ T-cells specific for different islet cell-associated epitopes using combinatorial MHC multimers. Diabetes *59*, 1721–1730.

Veres, A., Faust, A.L., Bushnell, H.L., Engquist, E.N., Kenty, J.H., Harb, G., Poh, Y.C., Sintov, E., Gürtler, M., Pagliuca, F.W., et al. (2019). Charting cellular identity during human in vitro β-cell differentiation. Nature *569*, 368–373.

Virostko, J., Williams, J., Hilmes, M., Bowman, C., Wright, J.J., Du, L., Kang, H., Russell, W.E., Powers, A.C., and Moore, D.J. (2019). Pancreas Volume Declines During the First Year After Diagnosis of Type 1 Diabetes and Exhibits Altered Diffusion at Disease Onset. Diabetes Care *42*, 248–257.

World Health Organization (2016). Global Report on Diabetes. https://www.who.int/diabetes/global-report/en/.

STAR★METHODS

KEY RESOURCES TABLE

REAGENT or RESOURCE	SOURCE	IDENTIFIER
Antibodies		
Rat anti-C-peptide	Developmental Studies Hybridoma Bank (DHSB)	GN-ID4, RRID:AB_2255626
Mouse anti-NKX6.1	DHSB	F55A12, RRID:AB_532379
Mouse anti-glucagon	Santa Cruz Biotech	Cat#SC-514592, RRID:AB_2629431
Donkey anti-rat 594	Life Technologies	Cat#A21209, RRID:AB_2535795
Donkey anti-mouse Alexa 647	Life Technologies	Cat#A31571, RRID:AB_162542
Donkey anti-rabbit Alexa 488	Life Technologies	Cat#A21206, RRID:AB_2535792
Donkey anti-rabbit Alexa 594	Life Technologies	Cat#A21209, RRID:AB_2535795
Donkey anti-rabbit Alexa 647	Life Technologies	Cat#A31573, RRID:AB_2536183
Donkey anti-goat Alexa 647	Life Technologies	Cat#A21447, RRID:AB_141844
Donkey anti-sheep Alexa 488	Life Technologies	Cat#A11015, RRID:AB_141362
Donkey anti-rat 488	Jackson Laboratories	Cat#712-546-153, RRID:AB_2340686
Donkey anti-rat 405	Abcam	Cat#ab175670, RRID:AB_11009056
Mouse Anti-HLA-ABC PE-conjugated	Biolegend	W6/32, Cat#311406, RRID:AB_314875
Mouse anti-HLA-E PE-conjugated	Biolegend	3D12, Cat#342603, RRID:AB_1659250
Mouse anti-HLA-DR APC-conjugated	Biolegend	L243, Cat#307610, RRID:AB_314688
Mouse anti-PD-L1 APC-conjugated	Biolegend	29E.2A3, Cat#329708, RRID:AB_940360
Mouse anti-CD3 PB-conjugated	Biolegend	UCHT1, Cat#300417, RRID:AB_493094
Mouse anti-CD8 PE-conjugated	Biolegend	T8-Leu2, Cat#344705, RRID:AB_1953243
Mouse anti-CD4 PE/Cy7-conjugated	Biolegend	RPA-T4, Cat#300511, RRID:AB_314079
Mouse anti-CD69 Alexa 647-conjugated	Biolegend	FN50, Cat#310918, RRID:AB_528871
Mouse anti-CD25 Alexa 700-conjugated	Biolegend	M-A251, Cat#356118, RRID:AB_2562168
Mouse anti-CD95/Fas APC-conjugated	eBioscience	DX2, Cat#17-0959-42, RRID:AB_10807091
Mouse anti-CD49a PE-conjugated	BD Biosciences	Cat#559596, RRID:AB_397288
Mouse anti-CD26 APC-conjugated	Miltenyi Biotech	Cat# 130-120-769, RRID:AB_2752189
Mouse anti-Oct4 Alexa 488-conjugated	BD PharMingen	Cat#560253, RRID:AB_1645304
Mouse anti-Sox2 PE-conjugated	BD PharMingen	Cat#560291, RRID:AB_1645334
Mouse anti-SSEA4 V450-conjugated	BD PharMingen	Cat#561156, RRID:AB_10896140
Mouse anti-TRA-1-60 (A647-conjugated	BD PharMingen	Cat#560850, RRID:AB_10565983
Rabbit anti-PERK	Cell Signaling Tech.	D11A8, Cat#5683S, RRID:AB_10841299
Rabbit anti-PDI	Cell Signaling Tech.	C81H6, Cat#3501S, RRID:AB_2156433
Rabbit anti-BIP	Cell Signaling Tech.	C50B12, Cat#3177S, RRID:AB_2119845
Rabbit anti-GAPDH	Abcam	Cat#ab181602, RRID:AB_2630358
Bacterial and Virus Strains		
lentiCRISPRv2	Broad institute	RRID: Addgene_52961
pHDM-vsvG, -tat, rev, gag/pol	Harvard Medical School DNA Resource Core	N/A
Sendai virus (SeV) Cytotune 2 kit	Life Technologies	Cat#A16517
Biological Samples		
Human peripheral blood	University of Massachusetts Medical School	N/A
Human Peripheral Blood Leukapheresis Pack	Stem Cell Technologies	Cat#70500.1
Lenti-X 293T Cell Line	Takara Bio	Cat#632180
Chemicals, Peptides, and Recombinant Proteins		
Activin A	R&D Systems	Cat#338-AC
Rock Inhibitor Y-27632	DNSK	Cat#DNSK-KI15-02

(*Continued on next page*)

Continued

REAGENT or RESOURCE	SOURCE	IDENTIFIER
Chir99021	Stemgent	Cat#04-0004-10
KGF	Peprotech	Cat#100-19
Retinoic acid	Sigma-Aldrich	Cat# R2625
LDN193189	Sigma-Aldrich	Cat#SML0559
Sant1	Sigma-Aldrich	Cat#S4572
PBDU	EMD Millipore	Cat#524390
XXI	EMD Millipore	Cat#565790
Alk5i II	Axxora	Cat#ALX-270-445
T3	EMD Millipore	Cat#642511
Betacellulin	ThermoFisher Scientific	Cat# 565790
Human IFN gamma	R&D Systems	Cat#285IF
Thapsigargin	Sigma-Aldrich	Cat#T9033
Critical Commercial Assays		
MSD U-PLEX Metabolic group 1 kit	MesoScale Discovery	Cat# K151ACM
STEMdiff Cardiomyocyte Differentiation Kit	Stem Cell Technologies	Cat# #05010
Experimental Models: Cell Lines		
Human iPSC-line T1D[1]	HSCI	iPSC 3107-001
Human iPSC-line T1D[2]	HSCI	iPSC 3107-002
Human iPSC-line T1D[3]	HSCI	iPSC 3107-003
Human iPSC-line ND	HSCI	iPSC 3107-013
Software and Algorithms		
QuantStudio 6 Flex Real-Time PCR system	Applied Biosystems	N/A
FlowJo v10	BD (Becton, Dickinson and Company)	N/A
GraphPad Prism8	GraphPad Software	N/A
nCounter	NanoString technologies	N/A

RESOURCE AVAILABILITY

Lead Contact

Further information and requests for resources and reagents should be directed to and will be fulfilled by the Lead Contact, Douglas A. Melton (dmelton@harvard.edu).

Materials Availability

This study did not generate any unique reagents. When appropriate, details and source information to synthesize non-commercially available intermediate chemicals are provided and original literature source cited. The corresponding author can be contacted for further details.

Data and Code Availability

The published report includes all data generated or analyzed during this study. No code was used or generated during this study.

EXPERIMENTAL MODEL AND SUBJECT DETAILS

All procedures were performed in accordance with the IRB guidelines at Harvard University and University of Massachusetts Medical School under IRB and ESCRO Protocols E00024. All iPSC lines were generated at the iPSC Core at Harvard Department of Stem Cells and Regenerative Biology.

METHOD DETAILS

iPSC and PBMCs Derivation from Human Donors

For iPSC derivation from blood, Sendai virus (SeV) Cytotune 2 kit (Life Technologies, Cat#A16517) was used to infect erythroblast-enriched populations following expansion. Briefly, 1×10^5 erythroblast-enriched populations were resuspended in 1mL of fresh

StemSpan SFEM II with Erythroid expansion supplement. After that, Sendai virus vectors were reconstituted at MOI of 5 for KOS, MOI of 5 for Myc and MOI of 3 for Klf4. Subsequently, virus suspension was added to the cells. On the following day cells were collected in a 15 mL falcon tube and washed with StemSpan SFEM II with Erythroid expansion supplement by centrifugation at 300 × g for 10 min. Two days post infection, cells were transferred from a well of a 12-well plate to a 6-well plate culture dish containing a mouse embryonic fibroblast (MEF) feeder layer and cultured further for 2 days in hES Media (mTeSR™1 - Stem Cell Technologies; 85850); subsequently, media were changed daily. At 15 to 21 days post transduction, the transduced cells began to form colonies with iPSC morphology, and visible colonies were handpicked and transferred onto 12-well plates.

Cell Culture

Human induced pluripotent stem-cell maintenance and differentiation were carried out as previously described (Pagliuca et al., 2014). Induced pluripotent stem-cell lines were obtained from stocks maintained by the Melton laboratory. Induced pluripotent stem cell lines were maintained in cluster suspension culture format using mTeSR3D (Stem Cell Technologies, 03950) in 500 mL spinner flasks (Corning, VWR) spinning at 70 rpm in an incubator at 37°C, 5% CO_2 and 100% humidity. Cells were passaged every 72h or 96h: induced human pluripotent stem-cell clusters were dissociated to single cells using gentle cell dissociation reagent (Stem Cell Technologies; 07174) and light mechanical disruption, counted and seeded at 0.7 M cells/ml in mTeSR3D + 10 μM Y27632 (DNSK International, DNSK-KI-15-02). Cell lines were authenticated by DNA fingerprinting, karyotyping (Cell Line Genetics) and all lines tested negative on routine mycoplasma contamination verifications. Differentiation flasks were started 72 h after passaging by replacing mTeSR3D medium with the appropriate differentiation medium including growth factors and small molecule supplements as previously described (Veres et al., 2019):

β Cell Differentiation Protocol

Stage 1: 24 hours in S1 medium supplemented with Activin A (100ng/ml), CHIR99021 (1.4 μg/ml) and Rock Inhibitor (10 μM), followed by 48 hours Activin A (100ng/ml) only.
Stage 2: 72 hours in S2 medium supplemented with KGF (50ng/ml) and Rock Inhibitor (10 μM).
Stage 3: 48 hours in S3 medium supplemented with KGF (50ng/ml), LDN193189 (200nM), Sant1 (0.25 μM), retinoic acid (2 μM), PBDU (500nM) and Rock Inhibitor (10 μM).
Stage 4: 5 days in S3 medium supplemented with KGF (50ng/ml), Sant1 (0.25 μM), retinoic acid (0.1 μM) and Rock Inhibitor (10 μM).
Stage 5: 7 days in BE5 medium supplemented with Betacellulin (20ng/ml), XXI (1 μM), Alk5i-II (10 μM) and T3 (1 μM). Sant1 (0.25 μM) was added in days 1 to 3, and retinoic acid was added at 0.1 μM in days 1 to 3, then at 0.025 μM.
Stage 6: 14-21 days in S3 medium, changed every 48h.

α Cell Differentiation Protocol

Stages 1-2: Same as β Cell Differentiation Protocol
Stage 3: 48 hours in S3 medium supplemented with LDN193189 (200nM), retinoic acid (2 μM) and Rock Inhibitor (10 μM).
Stage 4: 5 days in S3 medium supplemented with LDN193189 (200nM) and Rock Inhibitor (10 μM).
Stage 5: 7 days in S3 medium supplemented with Alk5i-II (10 μM).
Stage 6: 28 days in S3 medium supplemented with PBDU (500nM).

During feeds, the differentiating clusters were allowed to gravity-settle for 5–10 min, medium was aspirated and 300 mL of prewarmed medium was added. All experiments involving human cells were approved by the Harvard University IRB and ESCRO committees.

For cardiomyocyte differentiations, cells were seeded as clumps on 48 well plates and differentiated using the STEMdiff Cardiomyocyte Differentiation Kit (Stem Cell Technologies, 05010).

Magnetic enrichment using CD49a and CD26

Stage 6 clusters were dissociated using TrypLE Express for 20 min at 37°C. Cells were then quenched with DMEM + 10% FBS and spun down. Remaining undissociated cell clusters were mechanically dissociated using a P1000 pipette. The dissociated single cells were resuspended in sorting buffer (PBS + 1% BSA + 2 mM EDTA) and filtered through a 37-μm mesh filter. Cells were counted and resuspended at a density of 10 million cells per 300 μL in 15 mL conical tubes. Cells were stained at room temperature for 20 min using a 1:100 dilution of anti-human CD49a PE-conjugated (BD 559596) antibody, covered from light and agitated every 3 min. Stained cells were washed twice with 15 mL of sorting buffer by spinning down (5 min, 300 g) and resuspended to their initial density of 10 million cells per 300 μl. To label with microbeads, 40 μL of anti-PE UltraPure MACS microbreads (Miltenyi 130-105-639) were added for each 10 million cells, and the cell solution was incubated for 15 min at 4°C, agitated every 5 min. The stained cells were washed twice as above, and resuspended to a target density of 25–30 million cells per 500 μl. Volumes of 500 μL (containing no more than 30 million cells) were then magnetically separated on LS columns (Miltenyi 130-042-401) in a QuadroMACS separator (Miltenyi

130-090-976) using the recommended protocol. Successful PE enrichment was verified by live-cell flow cytometry on an Attune NxT (Invitrogen) flow cytometer. The negative cell fraction was stained at room temperature for 20 min using a 1:100 dilution of anti-human CD26 APC-conjugated (Miltenyi Biotech 130-120-769) antibody, stained cells were washed as above and incubated with anti-APC MACS microbreads (130-090-855). The cells were then magnetically separated on LS columns as described above.

Human Primary Immune Cell Isolation and Co-Culture Experiments

We obtained blood from Type 1 Diabetic (T1D) and non-diabetic (ND), de-identified donors from University of Massachusetts Medical School. For unmatched blood, fresh Leukopaks from human donors were purchased (Stem Cell Technologies, 70500.1). Human primary peripheral mononuclear cells (PBMCs) were isolated using the density gradient medium, Ficoll-Paque Plus (GE health care life sciences, 17144002) and the SepMate tubes (Stem Cell Technologies, 85450); T cells were isolated using EasySep Human T Cell Isolation Kit (Stem Cell Technologies, 17951). Isolated T cells were cultured in X-VIVO 10 (Lonza, 04-380Q) media supplemented with 5% Human AB Serum (Valley Biomedical, HP1022HI), 5% Fetal Bovine Serum (ThermoFisher Scientific, A3840101), 1% Penicillin/Streptomycin (ThermoFisher Scientific, 15070063), GlutaMAX (ThermoFisher Scientific, 35050061), MEM Non-Essential Amino Acids (ThermoFisher Scientific, 11140050).

T Cell Activation Assay

iPSC-β and α were used as target cells. Fifty to 100,000 target cells were plated on 96-well round bottom plates and treated with IFNγ, 100 ng/ml (Peprotech, 300-02) for 48h or thapsigargin, 5uM (Sigma Aldrich, T9033) for 5h before the assay. Cells were washed to remove residual thapsigargin and IFNγ. The immune/target cell ratio for co-culture is indicated in the figure legend. After a 48 hour co-culture, $CD4^+$ and $CD8^+$ T cells were stained for T cell activation markers CD69 and CD25. T cells activated with Dynabeads Human T-Activator CD3/CD28 beads (ThermoFisher Scientific, 111.61) for 48 hours were used as positive control. The results are presented as adjusted mean MFI, with the mean MFI of unstimulated PBMCs subtracted from the mean MFI of activation.

Flow cytometry

Intracellular Marker Staining

Differentiated clusters, sampled from suspension cultures (1–2 ml), were dissociated using TrypLE Express (GIBCO, 12604013) at 37°C, mechanically disrupted into single cells, fixed using 4% PFA for 30 min at room temperature and stored in PBS at 4°C. For staining, fixed single cells were incubated in Perm/Wash Buffer (BD Biosciences, 554723) for 30 min at room temperature, then incubated in Perm/Wash Buffer with primary antibodies (1 h at room temperature), washed three times with Perm/Wash Buffer, incubated with secondary antibodies in Perm/Wash Buffer (1 h at room temperature), washed three times and resuspended in Perm/Wash Buffer. Stained cells were analyzed using the Attune NxT (ThermoFisher) flow cytometer. A sample gating strategy is shown in Figure S1. Results presented in this study are representative of more than ten differentiations.

Surface Marker Staining

PBS containing 4% Fetal Bovine Serum (FBS) was used as blocking and staining buffer. Immune cells or other dissociated single cells were washed and blocked with blocking buffer for 30 min at 4°C, then incubated in blocking buffer with conjugated antibodies (1h at 4°C), washed three times with blocking buffer, fixed using 4% PFA for 30 min at room temperature and stored in PBS at 4°C. Stained cells were analyzed using the Attune NxT (ThermoFisher) flow cytometer.

Immunofluorescence Microscopy

Differentiated clusters were fixed in 4% PFA for 1 h at room temperature, washed, frozen in OCT (Tissue-Tek) and sectioned. For staining, slides were incubated in CAS block (ThermoFisher, 008120) with primary antibody overnight at 4°C, washed three times, incubated in secondary antibody for 2 h at room temperature, washed, mounted in ProLong Diamond Antifade Mountant with DAPI, covered with coverslips and sealed with clear nail polish. Representative regions were imaged using Zeiss.Z2 with Apotome or Zeiss Cell Discoverer 7 microscopes. Images shown are representative of similar results in at least three biologically separate differentiations from matched or similar stages.

Quantitative Real-time PCR (qPCR)

Cells were treated with TRIzol (ThermoFisher Scientific) for RNA extraction following the manufacturer's protocol. Purified RNA was reverse-transcribed into cDNA using the SuperScript IV first-strand synthesis kit (Invitrogen). GAD, PTPRN, G6PC2, SLC30A, IAPP and INS probes for TaqMan assays were purchased from ThermoFisher Scientific. All qPCR assays were performed using a QuantStudio 6 Flex Real-Time PCR system (Applied Biosystems).

NanoString gene array

Stage 6 cells from the β Cell Differentiation Protocol were enriched as described in the section 'Magnetic enrichment using CD49a and CD26.' Prior to the nanostring assay, the enriched populations, CD49a+ (iPSC-β) and CD26+ (iPSC-α) fractions were lysed using the RLT buffer (RNeasy Lysis Buffer, QIAGEN). An nCounter gene expression assay was performed according to the manufacturer's

protocol. The assay utilized a custom-made NanoString codeset designed to measure 24 transcripts, including 3 putative housekeeping transcripts (see Table S2). The data was normalized to the average counts for all housekeeping genes in each sample and analyzed with nSolver software (NanoString Technologies).

Protein Extraction and Immunoblotting

Cells were homogenized in RIPA buffer (ThermoFiscer, 89901) supplemented with protease and phosphatase inhibitors (Abcam, 201119). Total protein content was determined by BCA assay (ThermoFisher, 23225). Equal protein amounts (10 mg) were resolved by SDS-PAGE and transferred to nitrocellulose membranes (EMD Millipore). Membranes were immunoblotted with the indicated antibodies: PERK (Cell Signaling Technology, 5683S), PDI (Cell Signaling Technology, 3501S), BIP (Cell Signaling Technology, 3177S), GAPDH (Abcam, 181602).

Cytokines Analysis

Supernatant of co-culture experiments were assayed using the MSD proinflammatory custom panel, a highly sensitive multiplex enzyme-linked immunosorbent assay (ELISA) for quantitatively measuring cytokines including interferon γ (IFN-γ), interleukin (IL)-1β, IL-2, IL17, and C-X-C motif chemokine 10 (CXCL10) from the supernatants using an electrochemiluminescent detection method (MesoScale Discovery, Gaithersburg, MD, USA).

Viability and Apoptosis Assay

48h prior to co-culture with PBMCs, differentiated clusters were dissociated and reaggregated in V-bottom 96-well plates. PBMCs were then co-cultured to re-aggregated iPSC-islets, with and without 5h pre-treatment with 5uM thapsigargin (Sigma Aldrich, T9033). For live counts of iPSC-β or iPSC-α, clusters were dissociated, and single cells were fixed (1% paraformaldehyde) and stained with rat anti-C-peptide (DHSB, GN-ID4) and mouse anti-glucagon (Santa Cruz Biotech, SC-514592) antibodies for flow cytometry. For the apoptosis assay, clusters were dissociated, and single cells were stained at room temperature for 30 min using a 1:100 dilution of recently reported stem cell derived β-cell marker, anti-human CD49a (Veres et al., 2019) PE-conjugated (BD Biosciences, 559596), α-cell marker anti-human CD26 APC-conjugated (Miltenyi Biotech, 130-120-769), and Apopxin green indicator (Abcam, ab176750).

Lentivirus Preparation and Transduction

Lentiviral particles were produced by transfecting 293T cells (Takara Bio, Mountain View, CA, USA) with the packaging vectors pHDM-vsvg, pHDM-tat, pHDM-rev, and pHDM-gag/pol along with lentiviral backbone vectors using the TransIT-293 transfection reagent (Mirus, Madison, WI, USA). The following lentiviral vectors were used: non-targeting guide RNA (5′-TTTACGATC TAGCGGCGTAG-3′) or a B2M guide RNA (5′-GCTACTCTCTCTTTCTGGCC-3′) cloned into lentiCRISPRv2 [a gift from Feng Zhang (Addgene plasmid # 52961 ; http://addgene:52961; RRID:Addgene_52961 (Sanjana et al., 2014)]. Lentiviral particles were concentrated 48 h and 72 h post transfection using the PEG-IT virus precipitation reagent (Fisher Scientific, Waltham, MA, USA) overnight at 4°C followed by centrifugation at 1500 g for 30 min at 4°C and stored at −80°C. For transduction, cell clusters collected from spinner flask suspension cultures were dissociated in TrypLE Express (Life Technologies, Carlsbad, CA, USA) for 7 min, followed by mechanical dissociation and centrifugation at 300 g for 5 min at room temperature (RT). Cell pellets were resuspended at a density of 2.5 million cells/mL in the stage-matched medium with polybrene reagent (Santa Cruz, Dallas, TX, USA) at 8μg/mL. Single-cell suspensions were combined with concentrated lentiviral particles and plated on ultra-low attachment six-well plates on a rocker plate set at 70rpm in a humid 37°C incubator and 5% CO_2.

QUANTIFICATION AND STATISTICAL ANALYSIS

Statistical analyses are described in detail where reported. Statistical analyses were carried out using Graphpad Prism software. Statistical assays were performed as described in each figure legend. n represents number of biological replicates in all cases where reported. Biological replicates refer to unique donor-derived batches of human islets or unique differentiations of iPSC-derived cells produced from unique suspension cultures.

Cell Reports, Volume *32*

Supplemental Information

Modeling Type 1 Diabetes *In Vitro* Using Human Pluripotent Stem Cells

Nayara C. Leite, Elad Sintov, Torsten B. Meissner, Michael A. Brehm, Dale L. Greiner, David M. Harlan, and Douglas A. Melton

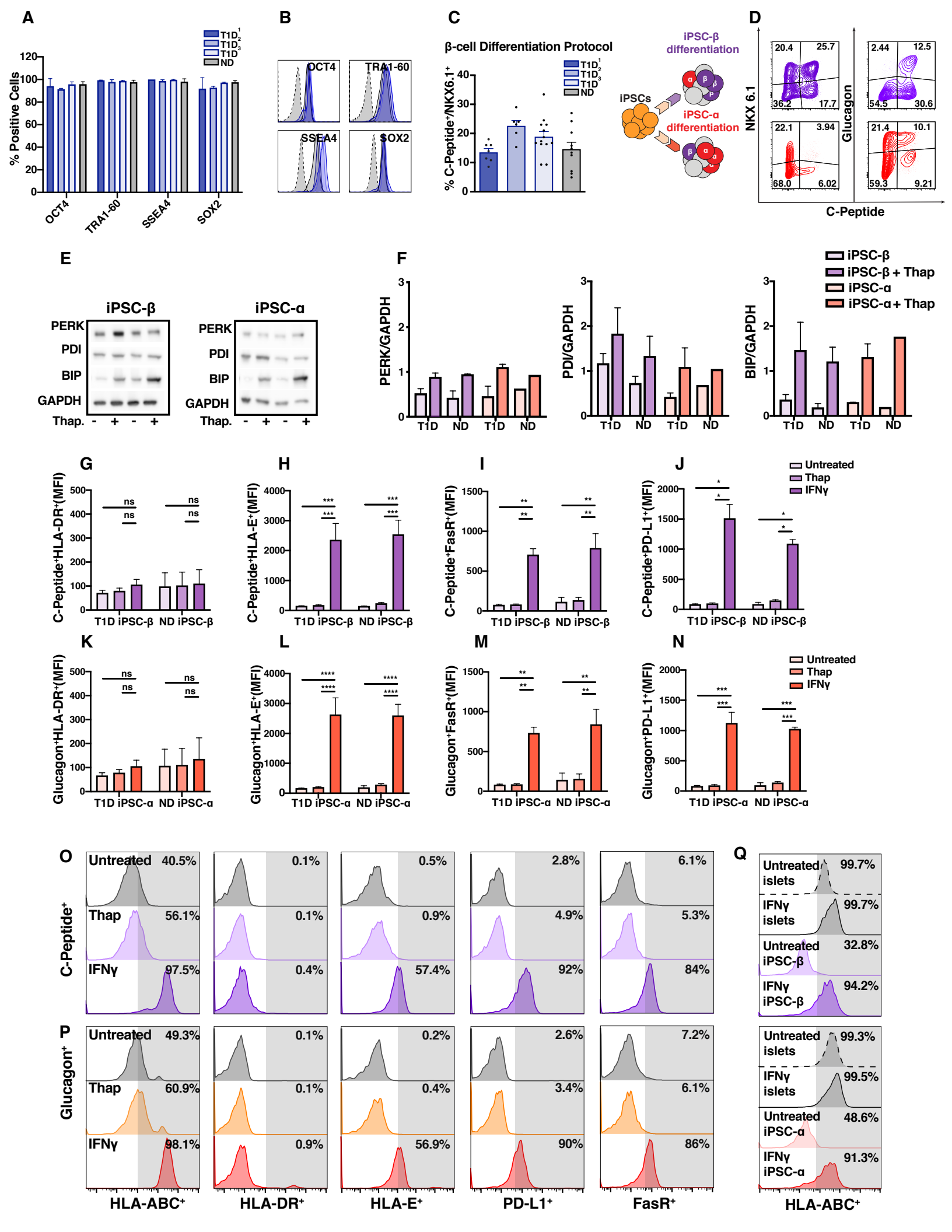
A
% Positive Cells
T1D1
T1D2
T1D3
T1D
ND
OCT4
TRA1-60
SSEA4
SOX2
B
OCT4
TRA1-60
SSEA4
SOX2
C
β-cell Differentiation Protocol
% C-Peptide+/NKX6.1+
iPSCs
iPSC-β differentiation
iPSC-α differentiation
D
NKX 6.1
Glucagon
C-Peptide
20.4
25.7
36.2
17.7
2.44
12.5
54.5
30.6
22.1
3.94
68.0
6.02
21.4
10.1
59.3
9.21
E
iPSC-β
iPSC-α
PERK
PDI
BIP
GAPDH
Thap. - + - +
F
iPSC-β
iPSC-β + Thap
iPSC-α
iPSC-α + Thap
PERK/GAPDH
PDI/GAPDH
BIP/GAPDH
T1D ND T1D ND
G
C-Peptide+HLA-DR+(MFI)
H
C-Peptide+HLA-E+(MFI)
I
C-Peptide+FasR+(MFI)
J
C-Peptide+PD-L1+(MFI)
Untreated
Thap
IFNγ
T1D iPSC-β ND iPSC-β
K
Glucagon+HLA-DR+(MFI)
L
Glucagon+HLA-E+(MFI)
M
Glucagon+FasR+(MFI)
N
Glucagon+PD-L1+(MFI)
T1D iPSC-α ND iPSC-α
O
C-Peptide+
Untreated 40.5% 0.1% 0.5% 2.8% 6.1%
Thap 56.1% 0.1% 0.9% 4.9% 5.3%
IFNγ 97.5% 0.4% 57.4% 92% 84%
P
Glucagon+
Untreated 49.3% 0.1% 0.2% 2.6% 7.2%
Thap 60.9% 0.1% 0.4% 3.4% 6.1%
IFNγ 98.1% 0.9% 56.9% 90% 86%
HLA-ABC+ HLA-DR+ HLA-E+ PD-L1+ FasR+
Q
Untreated islets 99.7%
IFNγ islets 99.7%
Untreated iPSC-β 32.8%
IFNγ iPSC-β 94.2%
Untreated islets 99.3%
IFNγ islets 99.5%
Untreated iPSC-α 48.6%
IFNγ iPSC-α 91.3%
HLA-ABC+

Figure S1. iPSC-β and iPSC-α are sensitive to ER-stress induction *in vitro*. Related to Figure 1.
(A-B) iPSC lines characterization.
(A) Flow cytometric analysis of pluripotent markers in iPSCs (n=3 T1D and n=1 iPSC ND donor, n=3 batches per donor line), quantification of positive cells for OCT4, TRA1-60, SSEA4, SOX2 in comparison to IgG isotype control.
(B) Representative flow cytometry histograms. Each color represents a different donor's iPSCs. Dashed histogram represents the IgG isotype control.
(C) Flow cytometry quantification of C-Peptide and NKX6.1 double positive cells in the iPSC-β protocol. Data are mean ± SEM. n=3 T1D iPSC donors and n=1 ND iPSCs line, n=3 to 7 differentiation batches per donor line.
(D) Representative flow cytometry plots for β and α cell markers, C-Peptide, NKX6.1 and glucagon in cells produced from the β cell differentiation protocol (top panels, as presented in the scheme S1D) or α cell differentiation protocol (bottom panels, as presented in the scheme S1D).
(E and F) Western blot analysis of PERK, PDI and BIP, in differentiated iPSC-derived endocrine cells (β or α as indicated), untreated or treated with thapsigargin (thap, 5μm for 5 h).
(F) Quantification of western blot analysis. n=3 T1D iPSC donors, n=1 iPSC ND donor, n=3 differentiation batches per donor line. $T1D^1$, $T1D^2$ and $T1D^3$ were pooled together. Data are mean ± SEM.
(G-N) Flow cytometry analysis gates of differentiated iPSC-derived endocrine cells treated with thap (5μm for 5 h) or IFNγ (100U/ml, 48h). Median fluorescence intensity (MFI) in (C-F) C-peptide positive or (G-J) glucagon positive cells, co-stained with (C and G) HLA-DR, (D and H) HLA-E, (E and I) FasR or (F and J) PD-L1. n=3 T1D iPSC donors, n=1 iPSC ND donor, n=3 batches per donor line. $T1D^1$, $T1D^2$ and $T1D^3$ were pooled together.
(O and P) Representative flow cytometry histograms gates of (K) C-peptide positive cells or (L) glucagon positive cells, co-stained with HLA-A, B, C, HLA-DR, HLA-E, PD-L1 or FasR.
(Q) Representative flow cytometry histograms gates of C-peptide positive cells (purple) or glucagon positive cells (red) of iPSC-β compared to human islets. (n=3 T1D iPSC donors, n=1 iPSC ND donor, n=1 differentiation batch per donor line).
**p<0.005, ***p<0.0005, ****p<0.0001 Ordinary one-way ANOVA. Data are mean ± SEM.

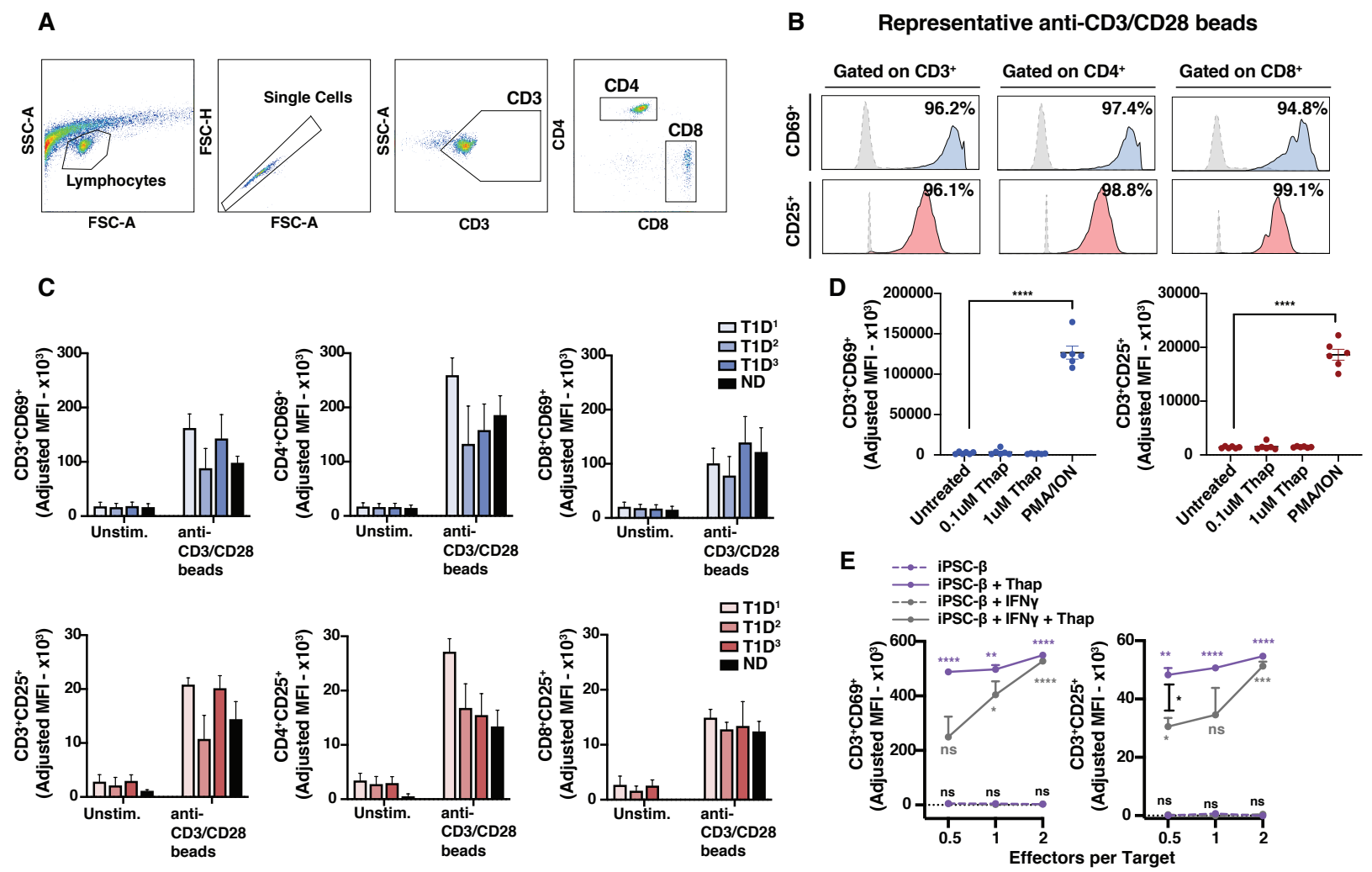

Gating strategy for Activation Assays

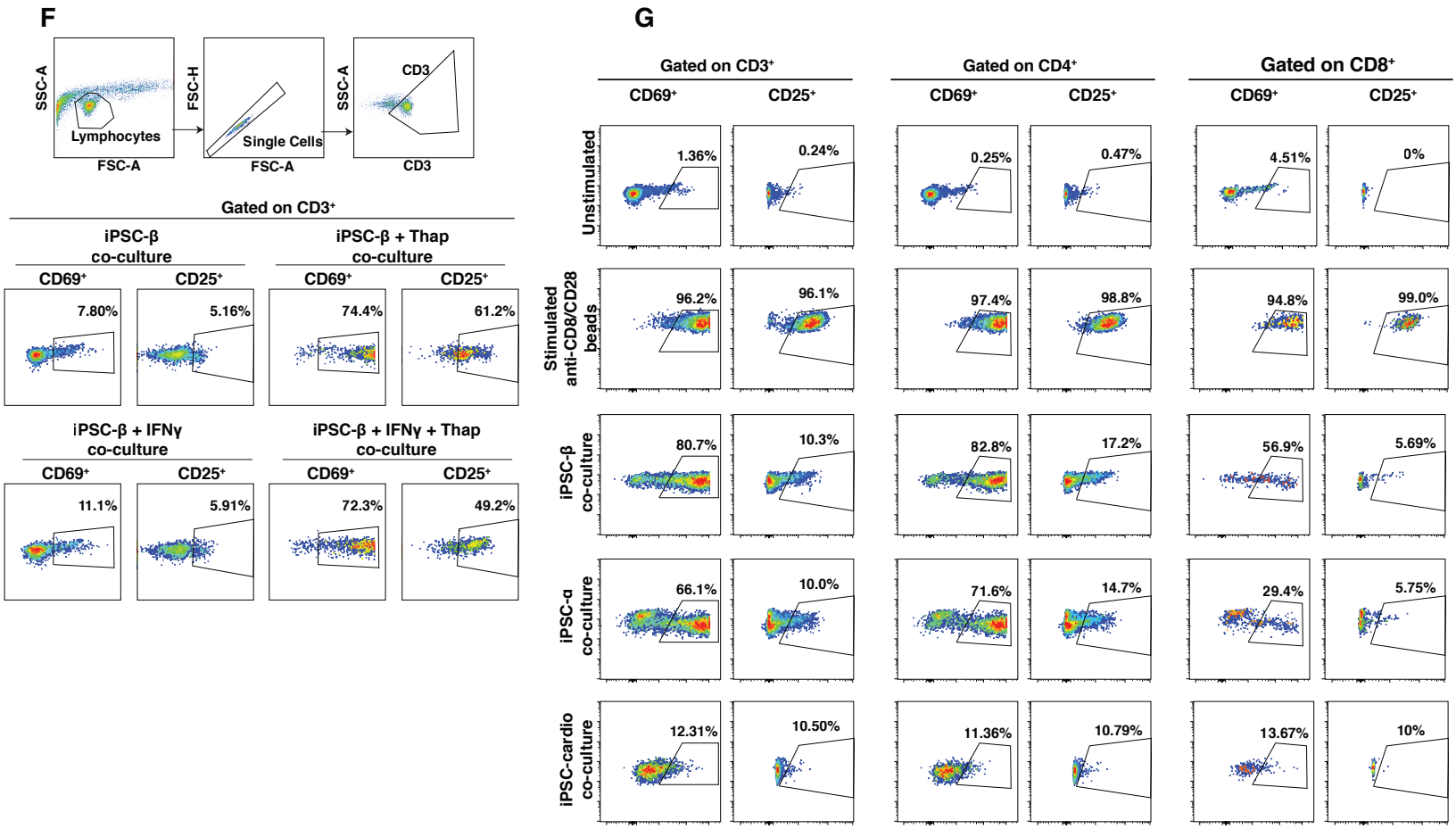

Figure S2. Positive and negative controls for the PBMCs activation assays. Related to Figure 2.
(A) Representative gating strategy for lymphocytes, single cells, $CD3^+$, and $CD4^+$ or $CD8^+$ cell populations; used in all T cell activation gating presented in Figures 2 to 4.
(B-C) Flow cytometry analysis of T cell activation markers, $CD25^+$ and $CD69^+$ on $CD3^+$, $CD4^+$ and $CD8^+$ populations activated with anti-CD3/anti-CD28 beads.
(B) Representative flow cytometry plots of $CD3^+$, $CD4^+$ and $CD8^+$ cells showed in B, expressing CD25 or CD69, unstimulated (gray histogram) or stimulated with anti-CD3/CD28 activation beads (in blue: CD69 and in red: CD25 positive control).
(C) PBMC negative and positive controls. Positive control stimulations were performed using anti-CD3/CD28 beads. Data are mean ± SEM.
(D) Flow cytometry representation of T cell activation markers, $CD25^+$ and $CD69^+$ on CD3 population from PBMCs treated with thap (0.1 or 1uM for 5h) or PMA/Ionomycin, as a positive control (n=3 T1D PBMCs preparation).
(E) Flow cytometry analysis of T cell activation markers after co-culture, gated on $CD3^+$ cells. Autologous PBMCs co-cultured with iPSC-β untreated or pre-treated with thap (5μm for 5 h) ± IFNγ (100U/ml for 48h) (n=1 T1D donor, n=3 differentiation batches per donor line.
$T1D^1$, $T1D^2$ and $T1D^3$ were pooled together).
(F) Representative gate strategy of data presented on E.
(G) Gating strategy for activation assays. Representative gating strategy for lymphocytes, single cells, $CD3^+$, and $CD4^+$ or $CD8^+$ cell populations, and activation markers CD25 and CD69; used in all T cell activation gating presented in Figures 2 and 4.
Data are mean ± SEM. *<0.05, **p<0.005, ***p<0.0005, ****p<0.0001 Two-way ANOVA: (E) Purple: thaps vs. untreated. Grey: Thap+IFNγ vs. IFNγ. Black: IFNγ vs. no IFNγ. ns, non-significant. Effector to target ratio are indicated.

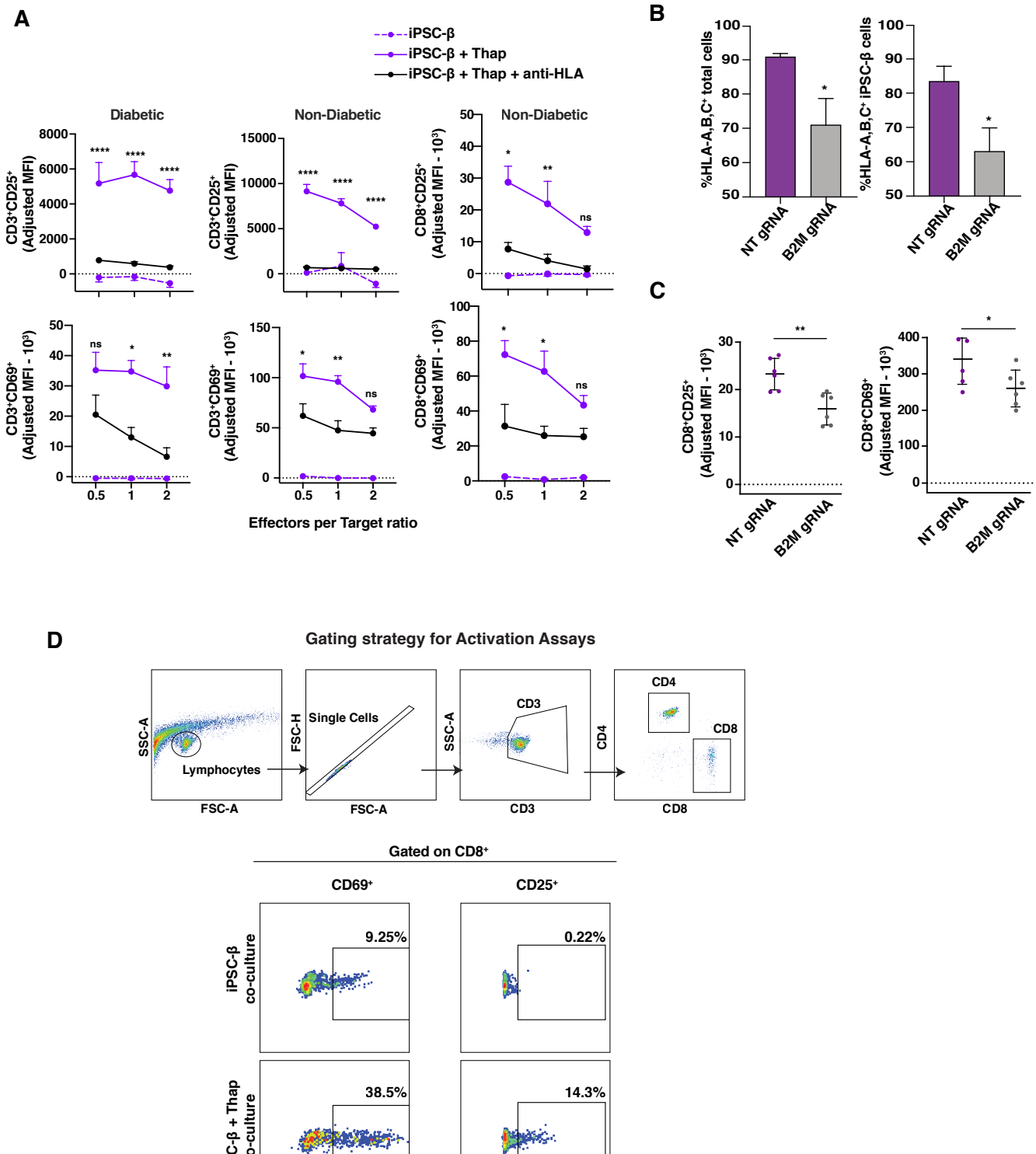
A
iPSC-β
iPSC-β + Thap
iPSC-β + Thap + anti-HLA
Diabetic
Non-Diabetic
Non-Diabetic
CD3+CD25+ (Adjusted MFI)
CD3+CD25+ (Adjusted MFI)
CD8+CD25+ (Adjusted MFI - 10³)
CD3+CD69+ (Adjusted MFI - 10³)
CD3+CD69+ (Adjusted MFI - 10³)
CD8+CD69+ (Adjusted MFI - 10³)
Effectors per Target ratio
B
%HLA-A,B,C+ total cells
%HLA-A,B,C- iPSC-β cells
NT gRNA
B2M gRNA
C
CD8+CD25+ (Adjusted MFI - 10³)
CD8+CD69+ (Adjusted MFI - 10³)
NT gRNA
B2M gRNA

D
Gating strategy for Activation Assays
SSC-A
Lymphocytes
FSC-A
FSC-H
Single Cells
FSC-A
SSC-A
CD3
CD3
CD4
CD4
CD8
CD8
Gated on CD8+
CD69+
CD25+
iPSC-β co-culture
9.25%
0.22%
iPSC-β + Thap co-culture
38.5%
14.3%
iPSC-β + Thap + anti-HLA co-culture
11.0%
0.54%

Figure S3. iPSC-β induced T cell activation is mediated by direct T cell-HLA interaction in T1D and ND donors. Related to Figure 3.

(A) PBMCs co-cultured for 48h with autologous iPSC-β (n=3 T1D donors, 3 differentiation batched per donor. $T1D^1$, $T1D^2$ and $T1D^3$ were pooled together) in increasing PBMCs to iPSC-β ratio. iPSC-β were untreated or pre-treated with thapsigargin (thap, 5μM for 5h) and/or anti-HLA antibody for 30min prior to co-culture. Flow cytometry analysis after co-culture of T cell activation markers, $CD25^+$ and $CD69^+$ on $CD3^+$ gated cells and $CD8^+$ gated cells as indicated.

Data are mean ± SEM. *p<0.05, **p<0.005, ***p<0.0005, ****p<0.0001. Two-way ANOVA. ns, non-significant. n=3 T1D iPSC donors, n=1 iPSC ND donor, n=3 batches per donor line. $T1D^1$, $T1D^2$ and $T1D^3$ were pooled together.

(B) Percentage of HLA-A, B, C^+ expression in total cells in iPSC-β differentiation and C-$peptide^+$/$glucagon^-$ cells (iPSC-β cells). Samples were collected 10 days after transduction with a lentivirus vector targeting beta 2 microglobulin (B2M) gRNA or non-targeting control gRNA and expressing Cas9.

(C) Expression of the activation marker CD25 (left) and CD69 (right) in $CD8^+$ gated cells after co-culture with autologous iPSC-β transduced with a lentivirus vector expressing a non-targeting or B2M gRNA and Cas9. n=1 ND iPSC donor, n=3 differentiation batches per donor line. $T1D^1$, $T1D^2$ and $T1D^3$ were pooled together. *p<0.05, **p<0.01, student t-test. Data are mean ± SEM.

(D) Representative gating strategy for lymphocytes, single cells, $CD3^+$, and $CD8^+$ cell populations, and activation markers CD25 and CD69; used in T cell activation gating presented in Figure 3.

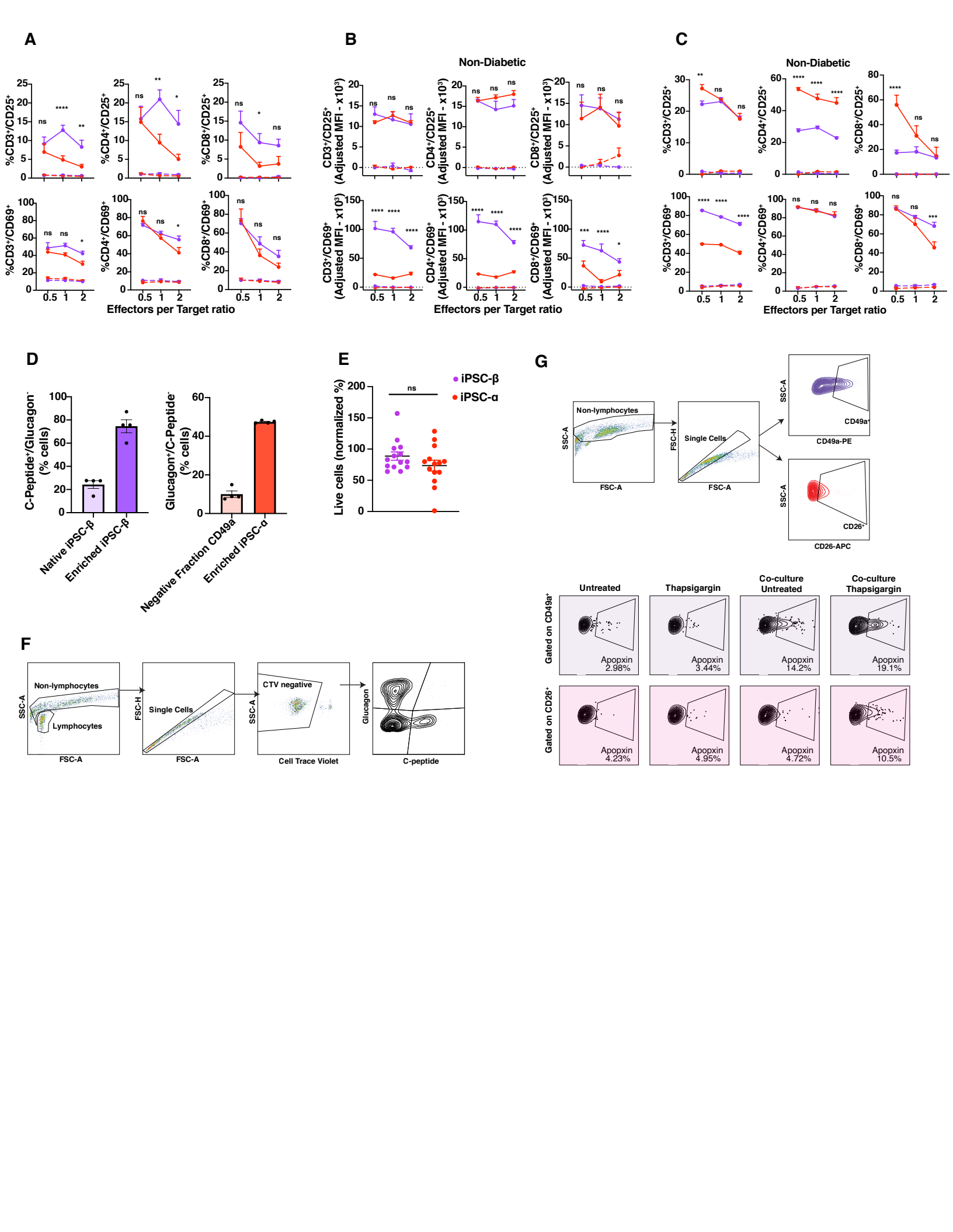
A
B
C
Non-Diabetic
Non-Diabetic
%CD3+/CD25+
%CD4+/CD25+
%CD8+/CD25+
%CD3+/CD69+
%CD4+/CD69+
%CD8+/CD69+
CD3+/CD25+ (Adjusted MFI - x10³)
CD4+/CD25+ (Adjusted MFI - x10³)
CD8+/CD25+ (Adjusted MFI - x10³)
CD3+/CD69+ (Adjusted MFI - x10³)
CD4+/CD69+ (Adjusted MFI - x10³)
CD8+/CD69+ (Adjusted MFI - x10³)
Effectors per Target ratio
Effectors per Target ratio
Effectors per Target ratio
D
C-Peptide+/Glucagon- (% cells)
Glucagon+/C-Peptide- (% cells)
Native iPSC-β
Enriched iPSC-β
Negative Fraction CD49a
Enriched iPSC-α
E
Live cells (normalized %)
iPSC-β
iPSC-α
ns
G
Non-lymphocytes
SSC-A
FSC-A
FSC-H
Single Cells
CD49a+
CD49a-PE
CD26-
CD26-APC
Untreated
Thapsigargin
Co-culture Untreated
Co-culture Thapsigargin
Gated on CD49a+
Gated on CD26+
Apopxin 2.98%
Apopxin 3.44%
Apopxin 14.2%
Apopxin 19.1%
Apopxin 4.23%
Apopxin 4.95%
Apopxin 4.72%
Apopxin 10.5%
F
Non-lymphocytes
Lymphocytes
SSC-A
FSC-A
FSC-H
Single Cells
CTV negative
Cell Trace Violet
Glucagon
C-peptide

Figure S4. Activation and killing by T cells is selective for iPSC-β in T1D and ND donors. Related to Figure 4.
(A-C) Cell surface T cell activation marker expression showed as (A and C) frequency or (B) MFI of $CD25^+$ or $CD69^+$ cells. Expression of the activation marker CD25 (top) and CD69 (bottom) on $CD3^+$, $CD4^+$ or $CD8^+$ gated T cells as indicated. PBMCs (gated on $CD3^+$, $CD4^+$ and $CD8^+$ populations) co-cultured with autologous iPSC-β or iPSC-α in increasing PBMCs:iPSC-β or iPSC-α ratios. (A) n=3 T1D iPSC donors, n=3 differentiation batches per donor line. $T1D^1$, $T1D^2$ and $T1D^3$ were pooled together. (B and C) n=1 ND iPSC donor, n=3 differentiation batches per donor line. Data are mean ± SEM. Two-way ANOVA. *p<0.05, **p<0.005, ***p<0.0005, ****p<0.0001, ns, not significant.
(D) Flow cytometry quantification of C-peptide and glucagon positive cells generated using the β differentiation protocol and enriched using CD49a and CD26 magnetic sorting. Percentage of enriched iPSC-β or iPSC-α cell populations are shown. n=1 T1D iPSC donor, n=3 differentiation batches per donor line.
(E) Percentage of live iPSC-β ($C\text{-peptide}^+/Glucagon^-$) or iPSC-α ($C\text{-peptide}^-/Glucagon^+$) from β or α differentiation protocols, treated with thap, and co-cultured with autologous PBMCs (2:1 effector to target ratio). Values are normalized from control wells without PBMCs. n=3 T1D. $T1D^1$, $T1D^2$ and $T1D^3$ were pooled together. Data are mean ± SEM. ns, not significant, student t-test.
(F) Representative gating strategy for acquiring absolute counts of live iPSC-β or iPSC-α after co-culture, gated for $C\text{-peptide}^+/Glucagon^-$ or $C\text{-peptide}^-/Glucagon^+$, respectively. Co-cultured PBMCs were stained with Cell Trace Violet (CTV) dye to distinguish from iPSC-β or iPSC-α.
(G) Gating strategy for apoptosis assay. Representative gating strategy for non-lymphocytes, single cells, $CD49a^+$, $CD26^+$, and $apopxin^+$.

Table S1. Patient samples. Related to figure 1.

Donor number	Age	Gender	Disease diagnosis	Age of diagnosis	BMI (CDC calculator)	HLA-A2	HLA risk alleles
T1D[1]	42	F	T1D	5	25.2	Positive	HLA-DR3, -DR4, -DQ8
T1D[2]	27	F	T1D	25	23.6	Positive	None
T1D[3]	44	M	T1D	25	26.4	Positive	HLA-DR3
ND	27	F	ND	N/A	21.4	Positive	None

Table S2. List of transcripts and target sequences used for Nanostring expression profiling. Related to STAR methods.

Gene Name	Accession	Position	Target Sequence
ARX	NM_139058.2	2622-2721	TGCACTCAGCGTGGTATGGTAAAAGTTTGTCCTCCCGTAGATTCTTACTGTGTTGTAGATACGGTAGGGTTCCTAGACAAATATTTATGTACTCAAGCCC
CHGA	NM_001275.3	293-392	CTGCGCCGGGCAAGTCACTGCGCTCCCTGTGAACAGCCCTATGAATAAAGGGGATACCGAGGTGATGAAATGCATCGTTGAGGTCATCTCCGACACACTT
GCG	NM_002054.2	296-395	TGGACTCCAGGCGTGCCCAAGATTTTGTGCAGTGGTTGATGAATACCAAGAGGAACAGGAATAACATTGCCAAACGTCACGATGAATTTGAGAGACATGC
INS	NM_000207.2	309-408	GGGTCCCTGCAGAAGCGTGGCATTGTGGAACAATGCTGTACCAGCATCTGCTCCCTCTACCAGCTGGAGAACTACTGCAACTAGACGCAGCCCGCAGGCA
NKX6-1	NM_006168.2	661-760	CTGGCCTGTACCCCTCATCAAGGATCCATTTTGTTGGACAAAGACGGGAAGAGAAAACACACGAGACCCACTTTTTCCGGACAGCAGATCTTCGCCCTGG
PDX1	NM_000209.3	414-513	GGGAGCCGAGCCGGGCGTCCTGGAGGAGCCCAACCGCGTCCAGCTGCCTTTCCCATGGATGAAGTCTACCAAAGCTCACGCGTGGAAAGGCCAGTGGGCA

SST	NM_001048.3	286-385	AGCTGCTGTCTGAACCCAACCAGACGGAGAATGATGCCCTGGA ACCTGAAGATCTGTCCCAGGCTGCTGAGCAGGATGAAATGAGG CTTGAGCTGCAGAG
ActB	NM_001101.2	1011-1110	TGCAGAAGGAGATCACTGCCCTGGCACCCAGCACAATGAAGAT CAAGATCATTGCTCCTCCTGAGCGCAAGTACTCCGTGTGGATC GGCGGCTCCATCCT
G6PC2 (IGRP)	NM_021176.2	693-792	ACGGCCAGTCTGGGCACATACCTGAAGACCAACCTCTTTCTCTT CCTGTTTGCAGTTGGCTTTTACCTGCTTCTTAGGGTGCTCAACA TTGACCTGCTGT
GAD1	NM_000817.2	576-675	CAAAGGACCAACAGCCTGGAAGAGAAGAGTCGCCTTGTGAGT GCCTTCAAGGAGAGGCAATCCTCCAAGAACCTGCTTTCCTGTG AAAACAGCGACCGGG
GAD2	NM_000818.2	1246-1345	TGTATGCCATGATGATCGCACGCTTTAAGATGTTCCCAGAAGT CAAGGAGAAAGGAATGGCTGCTCTTCCCAGGCTCATTGCCTTC ACGTCTGAACATAG
IAPP	NM_000415.1	311-410	ATTCTCTCATCTACCAACGTGGGATCCAATACATATGGCAAGA GGAATGCAGTAGAGGTTTTAAAGAGAGAGCCACTGAATTACTT GCCCCTTTAGAGGA
PTPRN (IA2)	NM_001199763.1	477-576	TTCTCCAACGCTTACAAGGTGTGCTCCGACAACTCATGTCCCAA GGATTGTCCTGGCACGATGACCTCACCCAGTATGTGATCTCTCA GGAGATGGAGCG
SLC30A8 (ZNT8)	NM_173851.2	2166-2265	CAGATGCAACCAATTCATTCAGTCCACGAGCATGATGTGAGCA CTGCTTTGTGCTAGACATTGGGCTTAGCATTGAAACTATAAAG AGGAATCAGACGCA